BECHTEL BETTIS, INC.
WEST MIFFLIN, PENNSYLVANIA
MATERIALS TECHNOLOGY

INFORMATION BRIEF

Title: Modeling of Fission Gas Release in UO_2

Author: M. H. Krohn

Date: JAN 2 3 2006

Summary:

A two-stage gas release model was examined to determine if it could provide a physically realistic and accurate model for fission gas release under Prometheus conditions. The single-stage Booth model [1], which is often used to calculate fission gas release, is considered to be oversimplified and not representative of the mechanisms that occur during fission gas release. Two-stage gas release models require saturation at the grain boundaries before gas is release, leading to a time delay in release of gases generated in the fuel. Two versions of a two-stage model developed by Forsberg and Massih [2] were implemented using Mathcad [3]. The original Forsberg and Massih model [2] and a modified version of the Forsberg and Massih model that is used in a commercially available fuel performance code (FRAPCON-3) [4] were examined. After an examination of these models, it is apparent that without further development and validation neither of these models should be used to calculate fission gas release under Prometheus-type conditions. There is too much uncertainty in the input parameters used in the models. In addition, the data used to tune the modified Forsberg and Massih model (FRAPCON-3) was collected under commercial reactor conditions, which will have higher fission rates relative to Prometheus conditions [4].

Introduction:

Fission gas release from uranium dioxide nuclear fuel pellets can result in catastrophic failures due to pressurization and rupture of the cladding. An understanding of how fission gas products behave under the operating conditions for a Prometheus Reactor is imperative to the proper design of fuel elements.

Because the fission products xenon and krypton are almost completely insoluble in the fuel and their normal state is gaseous, they tend to be rejected from the fuel and eventually contribute to the fuel pin atmosphere or precipitate as small pockets of gas within the fuel. Fission gas products released from the fuel will lead to an increase in the pressure within the fuel pin and could ultimately lead to the failure of the fuel element. If the fission gas is trapped as bubbles in the fuel, it will lead to an increase in fuel swelling as compared to swelling that would occur if the gas had remained dispersed on the atomic scale. The swelling associated with the precipitation of fission gases can lead to fuel-cladding contact, which can shorten the life of the element. The presence of gas bubbles in the fuel will also lead to a decrease in the fuel thermal conductivity which can lead to higher fuel temperatures relative to fully dense fuel.

During fissioning of ^{235}U, xenon (Xe) and krypton (Kr) are formed within the fuel. It is important to note that other gaseous species are produced during the fissioning of

U^{235}, but this document will focus on the gaseous fission products xenon and krypton. The fractional yield of Xe and Kr from the fissioning of U^{235} in a fast spectrum is estimated to be about 0.30[a]. Initially, these gases are atomically dispersed throughout the fuel. As the Xe and Kr gas atoms diffuse through the fuel, they can begin to cluster due to random encounters. These clusters continue to grow, leading to the formation of closed porosity in the fuel. Once these intragranular bubbles are formed they begin to act as traps for additional Xe and Kr gas atoms. In addition to this newly created porosity, the porosity that is originally present in the fuel after processing will also trap gas. The intragranular bubbles can also migrate thorough the fuel. Their motion can be random or directional and is dependent on the temperature, temperature gradient and stress state in the fuel.

Swelling and gas release are complementary phenomena that can lead to complex behavior in fuel [5]. If large amounts of gas are released from the fuel to the plenum there is less gas available for swelling. Conversely, low levels of gas release are usually associated with high swelling rates. The behavior of fission gas products is quite complex and varies relative to position within the fuel. This has been shown through examinations of commercial fuel rods at different radial positions [5]. Figure 1 shows a schematic of the different regions that can be found in commercial fuel pellets. It should be noted that the schematic representation shown in Figure 1 is of a fuel pellet that has undergone a high degree of restructuring. Under Prometheus conditions it is not likely that the fuel will form a columnar grain structure[6]. The following discussion is provided to give insight into the relationship between gas release and swelling. In the outer region of the fuel, which is relatively cool compared to the inner positions, (when temperatures in the region of interest are less than ~1400 K) the fission gases are relatively immobile. This leads to minimal gas release and swelling. In the intermediate radial position, which is characterized by equiaxed grain growth (when temperatures in the region of interest are between ~1400 K and ~1800 K), both the gas release from the fuel and the swelling of the fuel can be significant. Even though gas is released, an appreciable amount is retained within the fuel as bubbles. In the hot inner region, which may be characterized by columnar-grains when temperatures are greater than ~1800 K and the temperature gradients are larger than ~250 K/mm, nearly all the gas is released, leaving a relatively low concentration of gas to contribute to swelling.

In addition to being captured by closed intragranular porosity, gas atoms can be trapped by dislocations and grain boundaries. This process also can lead to the formation of bubbles. Depending on the temperatures and stresses within the fuel and the burnup of the fuel, the intragranular bubbles can migrate to grain boundaries. Bubbles associated with mobile defects also can be swept along with defect motion. As bubbles are swept along, they will continue to pick up gas atoms in the fuel. As irradiation continues, bubbles begin to grow on grain faces and edges. Due to differences between grain boundary energy and free surface energy, the bubbles that form at the grain boundaries are non-spherical [5]. Once a certain fraction of the

[a] Taken from fission product concentration estimated using a point depletion calculation with the ORIGEN-S code simulating operation over a 15 year core life. The calculation used ORIGEN-S library fast spectrum averaged cross sections and thermal fission product yields with constant power operation to 6% Fissions per Initial Fissile Atom (FIFA). (No fast fission fission product yields were included in the available ORIGEN-S library). The ORIGEN-S calculations account for the transmutation and decay of fission products after they are produced.

grain faces and edges are covered with bubbles, an interconnected network of tunnels will form, allowing gas to escape to external surfaces, i.e. plenum, central void, or crack surfaces. Fission fragments can interact with intra- and inter- granular bubbles and cause the gases contained within these bubbles to re-dissolve into the fuel. This re-solution of gas atoms increases the concentration of gas atoms atomically dispersed within the grain and reduces the concentration of gas atoms at the grain boundaries [5]. Table 1 provides a summary of the physical process that can affect gas release and Figure 2 is a schematic of these processes. An accurate model needs to capture the sequence of events described above.

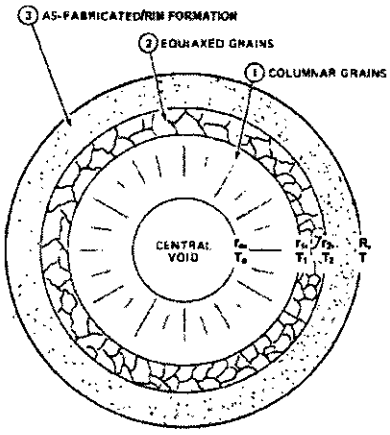

Figure 1 Different regions that can form in commercial UO_2 fuel pellets during irradiation [5].

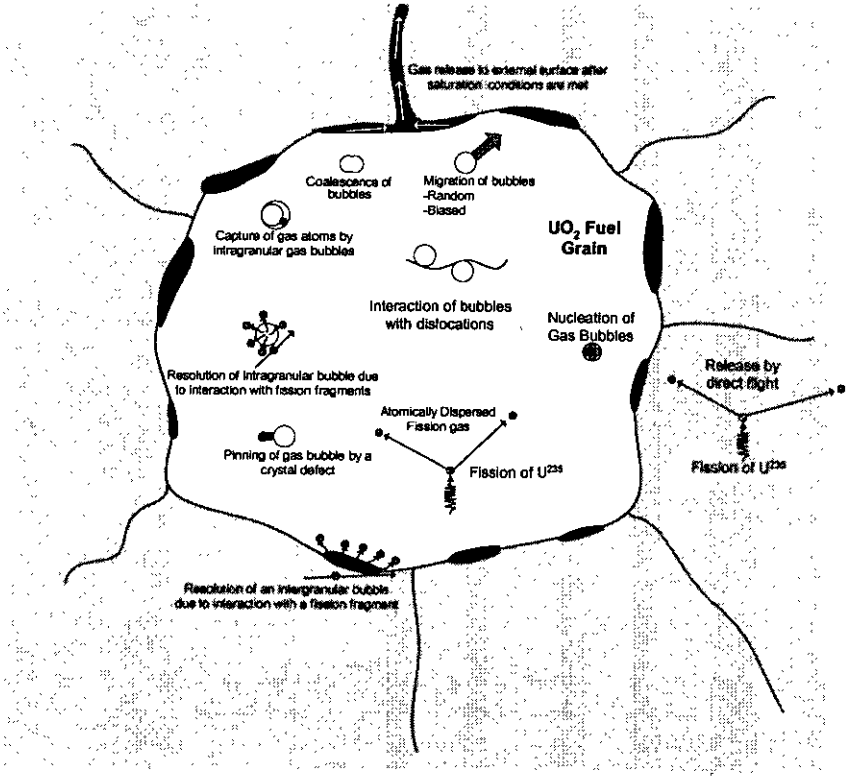

Figure 2 Schematic of the physical processes that can affect gas resolution.

Table 1 Physical Processes that Contribute to Fission Gas Release in Nuclear Fuels [5]

1) Production of xenon and krypton gasses by fission
2) Homogeneous and Heterogeneous nucleation of gas bubbles
3) Growth of gas bubbles, which can be affected by vacancy concentration, surface tension, and stress state in the fuel matrix
4) Re-solution of the gas atoms
5) Migration of bubbles
    a) Random walk process
    b) Biased motion
        i) Temperature and stress gradients cause bubbles to move in particular direction
        ii) Restraining forces due to dislocations and grain boundaries
            (1) Interaction can result bubbles to be pinned if the defect is immobile
            (2) Interaction can result in bubble being dragged if the defect is mobile
6) Coalescence of bubbles
7) Interaction of bubbles with crystal defects
8) Release of gas to either external (fuel cladding gap) and internal (grain boundaries) surfaces
9) Release of fission gas products by direct flight, which is significant only at low temperatures

In the late 1950's fission gas products were treated in the same manner as solid fission products [5]. This was an adequate approximation since the fission density, burn-up, and fuel temperatures in reactors at that time were too low to produce the complex phenomena that occur in fuels that operate under more severe conditions. Originally, gas release was treated using classical diffusion theory. The gas needed to diffuse through the fuel to an external surface before being released. The predicted release rates were lower than observed, revealing that it was incorrect to consider the fuel matrix to be grain free [5]. To account for the differences between the predicted and observed values, Booth adjusted the model by assuming the fuel was a collection of spheres [1]. Once gas atoms diffused to the surface of the sphere (which represents an idealized grain geometry), they were assumed to escape from the fuel. The size of the spheres could be adjusted to obtain agreement between the measured and calculated values of gas release. Although this topic is still debated, the success of the model lead to the theory that grain boundaries represented an easy path for gas release. Even with the application of the equivalent sphere model, there was still differences between the shapes of the measured release curves compared to release curves predicted from ordinary diffusion theory [5].

The departure of measured results from the predictions obtained from the Booth model lead to the notion that gas atoms can be trapped by radiation produced defects and natural defects in the fuel. Fission gas bubbles that form during reactor operation act as efficient traps for atomically dispersed gas atoms. Once a bubble has been nucleated it can continue to grow by absorbing more fission gases. The motion of these bubbles is much different than the diffusion of atomically dispersed gas atoms. Microstructural features within the fuel can pin gas bubbles and reduce their motion. In addition, irradiation can cause re-solution of fission gases into the fuel.

To properly characterize fission gas behavior, the following three quantities need to be determined as a function of position within the fuel and irradiation time [5]:

1) Concentration of gas dissolved in the fuel
2) Number and size distribution of intragranular and intergranular gas bubbles
3) Concentration of gas released from the fuel to an external surface

The sum of these three quantities is equal to the amount of gas produced during irradiation. In order to characterize these three quantities, the physical processes that contribute to fission gas behavior [5] must be described. However, even if all of the processes above could be described quantitatively, the physical variables necessary for these analyses are not well quantified, making it difficult to consider the results quantitatively. The variables that contribute to the behavior of fission gases in nuclear fuel are shown in Table 2 [5].

The assumptions of the Booth model for fission gas release are: the fuel is comprised of many equivalent spheres that do not change in size during irradiation; gas is created uniformly within the grain; gas that has diffused to the surface of the grain is released from the fuel. The diffusion equation that must be satisfied for all positions within the sphere is as follows [1]:

$$\frac{\partial c}{\partial t} = D\nabla^2 c + \beta \qquad (1)$$

with the initial conditions

$$c = 0 \quad \text{at } r = 0 \text{ to } a, \quad t = 0$$

and the boundary conditions

$$c = 0 \quad \text{at } r = a, \quad t \geq 0$$

$$\partial c/\partial r = 0 \quad \text{at } r = 0, \quad t \geq 0 \quad \text{(for symmetry)}$$

where D is the diffusion coefficient, which was assumed to be a constant to simplify the solution, c is the concentration, r is the radial position inside of the sphere, a is the radius of the spheres (grain), β is the generation rate, and t is time. The quantity

of gas released after a given amount of time can be determined by either integrating the divergent flux across the specimen or integrating the concentration profile. Both methods will give the following equation for fraction of gas released, f_c [1]:

$$f_c = 1 - \frac{6}{90\omega} + \frac{6}{\pi^4 \omega} \sum_{n=1}^{\infty} \frac{1}{n^4} e^{(-n^2 \pi^2 \omega)} \quad (2)$$

$$\text{where } \omega = Dt/a^2 \quad (3)$$

Table 2 Variables that Affect Fission Gas Behavior [5]

Temperature
Temperature gradient
Matrix stress
Matrix stress gradient
Fission Rate
Irradiation time or burnup
Fuel Properties Vapor pressure Surface tension Coefficient of thermal surface and bulk diffusion Creep strength
Fission gas properties Nuclear yields Equation of state Diffusion coefficient in the solid fuel Diffusion coefficient of the gaseous fuel
Fuel microstructure Dislocation density Grain size Restructuring Crack patterns
Condition of the fuel element, which determines the temperature profile and the state of stress in the fuel.

When $t \leq a^2/(\pi^2 D)$, corresponding to a gas release of up to 57%,the short time approximation for *Equation 2* is [1]:

$$f_c \approx 4\left(\frac{\omega}{\pi}\right)^{1/2} - \frac{3}{2}\omega \qquad (4)$$

Beyond 57% ($t > a^2/(\pi^2 D)$) the following approximation can be used [1]:

$$f_c \approx \frac{0.57}{\pi^2\omega} + 1 - \frac{1}{\pi^2\omega} - \frac{6e^{-1}}{\pi^4\omega} + \frac{6e^{-\pi^2\omega}}{\pi^4\omega} \qquad (5)$$

Speight considered the diffusion of fission gas products in a spherical grain of UO_2 that contained a fixed number of saturable gas atom traps [7]. The results showed that the Booth model for fission gas release can be extended to treat saturable traps within the fuel by using an effective diffusion coefficient, *D'*, defined by the following equation [7]:

$$D' = \frac{D \cdot b'}{b' + g} \qquad (6)$$

where *D* is the diffusion coefficient, *g* is the rate of absorption of gas atoms into the traps, and *b'* is the rate or resolution of gas atoms from the traps back into the fuel. The rate of absorption can be calculated using [8]:

$$g = 4\pi \cdot D \cdot r_b \cdot C_b \qquad \text{Eq7}$$

where r_b is the average bubble radius, and C_b is the bubble concentration. Equations for C_b and r_b were determined from empirical fits to data collected by Baker [9]:

$$r_b = 1.806\times10^{-9} \cdot \exp\left(1.039\times10^{-3} \cdot T\right) + 4.591\times10^{-11} \qquad (8)$$

$$C_b = \frac{9.98\times10^{28}}{T} - 1.42\times10^{23} \qquad (9)$$

The rate of resolution of an intragranular bubble can be calculated using:

$$b' = 3.03 \cdot F\pi \cdot l_f \cdot (r_b + Z_o) \qquad (10)$$

where *F* is the fission rate, l_f is the distance traveled by a fission fragment (6×10^{-6} m) [10], and Z_o is the range of influence of a fission fragment (10^{-9} m) [10]. The range of influence of a fission fragment is the distance from a fission fragment that a bubble can lie and still be destroyed. Using Equations 6 through 10, an effective diffusion coefficient can be calculated. This effective diffusion coefficient can be used in Equations 4 and 5 to calculate the fraction of gas released, taking into account gas trapping.

Turnbull [11] suggested that Equation 1 would take into account resolutions if the perfect sink boundary condition was changed to an imperfect sink boundary condition. This was accomplished by changing the boundary condition at the grain surface of the sphere:

$c = 0$ at $r = a$, $t \geq 0$ from Equation 1 to

$c = C'$ at $r = a$, $t \geq 0$ where:

$$C' = \frac{b_{gb} \cdot \lambda \cdot N}{2 \cdot D'} \tag{11}$$

where λ is the resolution depth of a bubble, N is the number of atoms per unit area of grain boundary, b_{gb} is the rate of resolution of an intergranular bubble, and D' is the effective diffusion coefficient. Equation 11 is based on the balance between diffusion flux and resolution [7]. Solving Equation 1 using the boundary condition described by Equation 11 gives the following equation [11]:

$$f_c = 1 - \frac{6}{\beta \cdot t} \sum_{n=1}^{\infty} \left[\frac{\beta \cdot a^2}{D(n\pi)^4} - \frac{C_o - C'}{(n\pi)^2} \right] \cdot \left[1 - \exp\left(\frac{-n^2 \pi^2 D \cdot t}{a^2} \right) \right] \tag{12}$$

This equation derived by Turnbull suggest that resolution becomes unimportant when the concentration close to the grain boundary, C', becomes insignificant in comparison with the concentration generated throughout the grain, βt [11]. When C_o=C'=0 Equation 12 reduces to the Booth equation.

Forsberg and Massih [2] extended the derivation of Turnbull [11] by modifying the boundary condition C' , defined by Equation 11, so that it varied with time (t):

$$C'(t) = \frac{b_{gb}(t) \cdot \lambda \cdot N(t)}{2 \cdot D(t)} \tag{13}$$

Using a numerical method, Forsberg and Massih [2] derived the following equations for the change in the number of gas atoms per unit volume of fuel within the grain, ΔG_o, and the change in the number of gas atoms per unit volume of fuel on the grain boundary, ΔG_b:

$$\Delta G_O = \sum_{n=1}^{3} \left[f_n G_n(\tau_1) + A_n \int_{\tau_1}^{\tau_2} \exp\left(-\frac{B_n}{a^2} (\tau_1 - \tau) \right) \cdot q(\tau) d\tau \right] \tag{14}$$

and

$$\Delta G_B = -\sum_{n=1}^{3} f_n G_n(\tau_1) + \int_{\tau_1}^{\tau_2} \left[\frac{6}{\sqrt{\pi}} \left(\frac{\tau_2 - \tau}{a^2} \right)^{1/2} - 3 \left(\frac{\tau_2 - \tau}{a^2} \right) \right] \cdot q(\tau) d\tau \tag{15}$$

where a is the radius of the grains, and τ, q, $G_n(\tau)$, and f_n are defined by the following equations:

$$\tau = \int_0^t D'(t)dt \tag{16}$$

where $D'(t)$ is the effective diffusion coefficient and t is time. The integration of the diffusion coefficient (Equation 16) is done to simplify the partial differential equation (Equation 1).

$$a^2 q(\tau)\cdot\left[-\sum_{n=1}^{3}\frac{f_n A_n}{B_n}+(1+h_4\beta_e(\tau_2))\cdot\left[\frac{4}{\sqrt{\pi}}\left(\frac{\Delta\tau}{a^2}\right)^{3/2}-\frac{3}{2}\left(\frac{\Delta\tau}{a^2}\right)^2\right]\right]= \tag{17}$$
$$\frac{1}{2}[\beta(\tau_1)+\beta(\tau_2)]\Delta t - h_4 G_B(\tau_1)\Delta\beta_e + h_4\beta_e(\tau_2)\sum_{n=1}^{3} f_n G_n(\tau_1)$$

$$G_n(\tau) = A_n\int_0^{\tau_m}\exp\left(-\frac{B_n}{a^2}(\tau_m-\tau)\right)\cdot q(\tau)d\tau \tag{18}$$

$$f_n = \exp\left(-\frac{B_n}{a^2}\Delta\tau\right)-1 \tag{19}$$

where β_e and h_4 can be calculated from:

$$\beta_e = \frac{\beta}{D'} \tag{20}$$

$$h_4 = \frac{a\cdot b_{gb}\cdot\lambda}{3\cdot\beta} \tag{21}$$

β is the gas production rate, D' is the effective diffusion coefficient, a is the grain radius, b_{gb} is the rate of resolution of an intergranular bubble, λ is the resolution depth.

A_n and B_n are as follows:

$$A_1 = 0.63003 \qquad B_1 = 9.9904$$
$$A_2 = 0.20651 \qquad B_2 = 64.488$$
$$A_3 = 0.14776 \qquad B_3 = 511.61$$

The values are based on the following approximation [2]:

$$2-\frac{6}{\pi^2}\cdot\sum_{n=1}^{\infty}\frac{\exp\left(\frac{-n^2\pi^2\tau}{a_o^2}\right)}{n^2}\approx\sum_{n=1}^{3}A_n\cdot\exp\left(-\frac{B_n}{a_o^2}\cdot\tau\right) \tag{22}$$

The numerical treatment used by Forsberg and Massih [2] to derive Equations 14, 15, and 17 assumes that ratio of the resolution rate to the production rate, b_{gb}/β, is a constant and that q is constant over the interval $\Delta\tau$. The concentrations of gas atoms can be determined using an iterative process; i.e., gas concentrations are calculated using q, and then a new q is determined using these gas concentrations. The gas concentration is zero at time zero. The Forsberg and Massih model is a two-stage model that requires gas saturation at the grain boundary before gas can be released. The gas in the fuel is released when the concentration on the grain boundary, G_b, is equal to the saturation concentration G_s. This can be determined using the following equations [2]:

$$G_S = \frac{3 \cdot N_s}{2 \cdot a} \tag{23}$$

$$N_s = \frac{4 \cdot r \cdot f(\theta) \cdot V_c}{3 \cdot k_b \cdot T \cdot \sin^2 \theta}\left(\frac{2\gamma}{\mathrm{r}} + P_{ext}\right) \tag{24 [12]}$$

$$f(\theta) = 1 - \frac{3\cos(\theta)}{2} + \frac{\cos^3(\theta)}{2} \tag{25}$$

where r is the projected radius of bubble at the grain boundary, $f(\theta)$ is a geometric factor*($\theta = 50^\circ$ based on the work of Reynolds et al. [13])*, V_C is the fraction of grain boundary surface area that is covered at saturation, T is the temperature (K), k_b is Boltzmann's constant (J/K). To calculate N_s (Equation 24) the fractional coverage of grain boundaries at saturation, V_c, and the projected radius of a grain boundary bubble, r, need to be specified. It has been observed that swelling on the grain faces saturates when the factional coverage is around 0.25 and the bubbles have a projected radius of 0.5 μm [10].

The standard commercial fuel performance code,FRAPCON-3, uses a modified version of the Forsberg and Massih equations [2] to calculated fission gas release. The modifications to the Forsberg and Massih model allow the FRAPCON-3 fission gas release model to circumvent deficiencies present in the Forsberg and Massih model while retaining its efficient solution algorithm [14].

The goal of this work was to gain an understanding of the original and modified Forsberg and Massih gas release models to determine if they could be used to calculate fission gas release under Prometheus conditions. A Prometheus reactor is expected to have a fast neutron spectrum (> 1 MeV) of ~100 x 10^{20} n/cm^2, a low fission rate 1-3 x 10^{12} f/cc-sec, an EOL burnup of 10-15 x 10^{22} fissions/cm^3 UO_2, a peak fuel temperature between 1200 to 1800 K, and operate for 15 effective full power years [6].

Analytical Procedures:

A program to calculate fission gas release based on the Forsberg and Massih [2] model was developed using Mathcad (Appendix 1). The program calculates the fraction of gas release and time for gas release to occur given a temperature profile and fission rate. Fission rates are manually set by the user or calculated based on fissions per initial metal atoms (FIMA) or fissions per initial fissile atoms (FIFA). As an output the program calculates the fraction of gas released using the Booth, Forsberg/Massih, and FRAPCON-3 models.

The program requires the user to put in the fuel characteristics, fuel temperature, amount of time that the fuel is at temperature, and the time step. The program proceeds in an iterative process, comparing the concentration of gas at the grain boundary to the saturation concentration. If the concentration at the grain boundary is equal to the saturation concentration, all of the gas is released. The concentration at the grain boundary goes to zero and the process begins again. Another approach would have been to continue to release the gas arriving at the grain boundaries once saturation conditions were met. Closing the tunnels after gas release was used in the program to be consistent with the FRAPCON-3 model.

After reviewing the FRAPCON-3 literature [4, 14] and speaking to a Pacific Northwest National Laboratory (PNNL) engineer [15], it was apparent that issues were encountered while developing the gas release portion of FRAPCON-3. First, in the Forsberg and Massih model, the gas that is redissolved is not available for diffusion or release [14]. To circumvent this issue the FRAPCON-3 model assumes that all the gas that is redissolved is released once saturation at the grain boundary is reached. Second, Forsberg and Massih [16] use a resolution parameter that is inversely proportional to the diffusion coefficient; the FRAPCON-3 developers found that at temperatures typical of the outer regions of commercial fuel pellets the resolution gas inventory becomes unrealistically large [14]. The solution was to tune the model to fit experimental data using fitting parameters. The diffusion coefficient and resolution parameters were multiplied by constants to tune the model [4]. In addition to these modifications, PNNL also modified the model by treating resolution separately.

It is important to note that the FRAPCON-3 model is a highly tuned model. The model was fit to data collected from commercial fuel rods and test assemblies that were design to mimic commercial fuel rods. The FRAPCON-3 literature indicates that the fission gas release model, valid over a temperature range of 300 K – 2300 K and a burnup range of 0 to ~6.5 %FIMA, is applicable for the burnup and temperature ranges expected for a Prometheus reactor. However, the fission rate under Prometheus conditions [~5×10^{11} to 2×10^{12} fissions per cubic centimeter uranium per second (f/cc(U)/s)] would be lower than fission rates of commercial reactors (typical pressurized water reactor fission rates are 1×10^{13} to 3×10^{13} f/cc(U)/s) that could affect the release of fission gases. Carroll et al. [17, 18] showed that for single crystal UO_2 at a constant temperature gas release is affected by fission rate. At 1673 K, the gas release for a fission rate of 5×10^{11} f/cc(U)/s compared to a fission rate of 1×10^{13} f/cc(U)/s would be roughly an order of magnitude higher[17, 18]. The

difference in gas release was related to the formation of defects during irradiation that act as gas traps [17, 18]. At low fission rates, the traps have a small effect relative to natural traps. The overall effect of fission-created traps on gas release increases as the fission rate increases. This is due to an increase in the number density of the traps. As the fission rate continues to increase a point is reached where fission tracks begin to annihilate traps that were created in previous fissions. Because of the relatively low fission rates expected under Prometheus conditions, the results calculated using the FRAPCON-3 model could differ significantly from gas release under Prometheus conditions. Before the model can be used, it would need to be verified and re-tuned. The data need to tune the model would need to be collected from specimens exposed to fission rates and conditions representative of Prometheus conditions. In addition, the issues discussed above suggest that data collected under accelerated fuel pin test may not be applicable for the design of low fission rate, long life fuel pins.

The change in the concentration of gas in the grain, ΔG_o, and on the boundary, ΔG_b, are calculated using the following equations [4]:

$$\Delta G_O = \sum_{n=1}^{3}\left[f_n G_n(\tau_1) + A_n \int_{\tau_1}^{\tau_2} \exp\left(-\frac{B_n}{a^2}(\tau_t - \tau)\right) \cdot q(\tau) d\tau \right] \tag{25}$$

$$\Delta G_B = -\sum_{n=1}^{3} f_n G_n(\tau_1) + \int_{\tau_1}^{\tau_2} funct(\tau_2 - \tau) \cdot q(\tau) d\tau \tag{26}$$

$$a^2 q \cdot \left[-\sum_{n=1}^{3} \frac{f_n A_n}{B_n} + \int_{\tau_1}^{\tau_2} funct(\tau_2 - \tau) d\tau \right] = \beta \Delta t \tag{27}$$

where

$$funct(\Delta\tau) = \frac{6}{\sqrt{\pi}}\left(\frac{\Delta\tau}{a^2}\right)^{1/2} - \frac{3}{2}\left(\frac{\Delta\tau}{a^2}\right) \quad \text{if } \tau < 0.1 \tag{28}$$

$$funct(\Delta\tau) = 1 - \frac{6}{\pi^2}\exp\left(\frac{-\pi \cdot \Delta\tau}{a^2}\right) \quad \text{if } \tau > 0.1 \tag{29}$$

G_n, f_n, A_n, B_n, τ, t, a, q, and β are defined in the previous section.

Resolution is introduced separately by defining the amount of gas arriving at grain boundary during each iteration as follows [4]:

$$\Delta \mathrm{Re}solvedGas = \frac{F}{1+F} \cdot \Delta G_B \tag{30}$$

$$\Delta G_B(After\ \mathrm{Re}solution) = \frac{\Delta G_B}{1+F} \tag{31}$$

where

$$F = FitMult\left(\frac{1.84\times10^{-14}\cdot a}{3\cdot D}\right) \qquad (32)$$

where *a* is the grain radius, and *D* is the diffusion coefficient. *FitMult* is a multiplier used for optimization by PNNL (*FitMult= 300*) while the term in the parenthesis is the term used by Forsberg and Massih ($h_4{}^*\beta_e$, Eq20 and 21) to describe resolution [2]. Equations 25 through 32 were entered into Mathcad and used to solve for gas release. In FRAPCON-3, the gas at the grain boundary and all of the resolved gas is released once saturation conditions are met.

Results:

Table 3 gives a list of the variables used for the fission gas release calculations. The range of influence of a fission fragment, Z_o,(Figure 3) is based on an approximation made by Turnbull [19]. He estimated it to be roughly 1 nm. The mechanism by which a bubble is destroyed is still a subject of debate, but one of the leading mechanisms is based on fission fragment energy lost via electron excitation [19]. The bubbles are destroyed due to a thermo-elastic stress pulse, which is a result of a cylindrical heat distribution around the fission fragment track [19]. This electron excitation mechanism implies that resolution is dependent on bubble size. Therefore, the efficiency by which a small intragranular bubble is destroyed be will different than a large intergranular bubble [19]. In addition, this mechanism also implies that resolution is related to the thermal and electrical conductivities of the fuel.

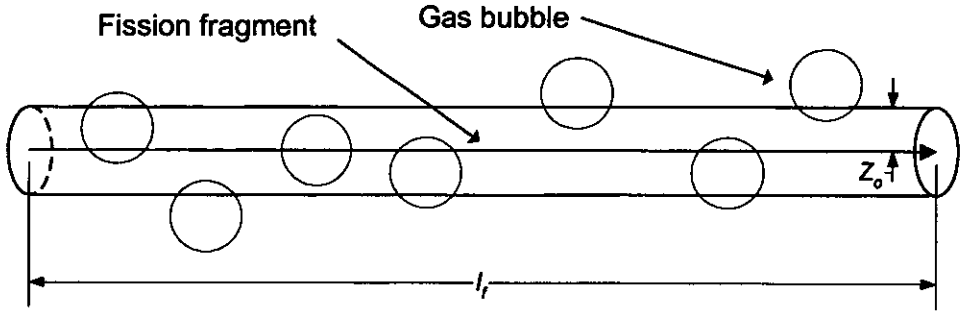

Figure 3 Schematic representation of the range of influence of a fission fragment, Z_o, and the distance traveled by a fission fragment, l_f, which are used in Equation 10 to calculate the rate of resolution of intragranular bubbles [5].

Table 3 Variables used to calculate fission gas release

Variable	Description	Value	Comments
T	Temperature	User defined	
F	Fission rate	Calculated	Based on burnup and enrichment
β	Production rate	0.3 F	
D_{int}	Diffusion coefficient	Literature	Empirical fit to data [2]
D_{eff}	Effective diffusion coefficient	Calculated (Eq6)	Takes into account trapping and resolution
l_f	Average fission fragment length	6×10^{-6} m	Taken from White and Tucker [10]
Z_o	Fission fragment range of influence	$\sim 10^{-9}$ m	Taken from White and Tucker [10]
λ	Resolution depth	$\sim 10^{-8}$ m	Taken from White and Tucker [10]
a_o	Radius of grain	User defined	
γ	Surface energy	0.6 J/m^2	Taken from Olander [5]
r_{gb}	Grain boundary bubble radius	5×10^{-7} m	Projected radius taken from White and Tucker [10]
$f(\theta)$	Shape factor for lenticular bubbles	Eq 24	Relates volume of lens to a complete sphere [10]
θ	Dihedral angle for lenticular bubbles	50°	Taken from White and Tucker [10]
V_c	Fractional coverage of grain boundary at saturation	0.25	Taken from White and Tucker [10]
C_b	Total gas bubble density	Eq9	Empirical fit to Baker's data [9]
r_b	Mean radius of intragranular bubble	Eq8	Empirical fit to Baker's data [9]
g	Gas atom absorption rate for intragranular bubbles	Eq7	Taken from White and Tucker [10]
b	Resolution probability of intragranular bubble	Eq10	Taken from White and Tucker [10]
b_{gb}	Resolution probability of grain boundary bubble	2×10^{-5} s^{-1}	Taken from White and Tucker [10]

The distance traveled by a fission fragment, l_f, is reported to be about 6 μm for most nuclear fuels [10]. The resolution depth from the grain boundary, λ, is estimated to be no more than 10 nm based on estimates of energies that would be transferred from a fission fragment to gas atoms during a collision [5].

The free surface energy for UO_2 is likely to lie between 0.3 and 0.7 J/m^2 [10]. A value of 0.6 J/m^2 was estimated by Olander and is used in these calculations [20].

The projected radius of a gas bubble on a grain boundary, r_{gb}, is estimated to be roughly 500 nm [10]. The probability that a gas bubble situated on a grain boundary undergoes resolution, b_{gb}, is unlikely to be as large as the probability of resolution of an intragranular bubble, b' [10]. This is consistent with the destruction of bubbles via the electron excitation mechanism discuss above [19]. White and Tucker [10] suggested that the probably of a bubble on the grain boundary undergoing resolution may be around 1% of the probability of an intragranular bubble undergoing resolution, b' that gives a value on the order of 1-2 x 10^{-5} s^{-1} [10]. This would result in the product of $b_{gb}\lambda$, being roughly 10^{-13} m/s. FRAPCON-3 refers to the term $b_{gb}\lambda$ as the original Forsberg and Massih resolution parameter and reports a value of 1.84 x10^{-14} [4, 14]. It is an order of magnitude lower than what has been suggested by White and Tucker [10]. This parameter can greatly affect the results and will be discussed in detail below.

The values for intragranular bubble concentration, C_b, and radius, r_b, are based on empirical fits to data reported by Baker [9]. These data were collected by examining thin sections of irradiated UO_2 fuel using SEM and TEM microscopy. The sections were taken from different regions of the fuel that were at different temperatures during irradiation. The fuel pins were irradiated to a burnup of ~1%, at temperatures ranging from 400- 2300°C, and at a rating of 25-46 watt/gram [9]. The results of Baker have been questioned [21]; however, since this data was used by Forsberg and Massih [22], it was used in these calculations.

The diffusion coefficients reported by Forsberg and Massih [2], which were referenced to data reported in a series of papers by Turnbull and Friskney [23-25] are as follows:

$$D_3 = 1.51\times10^{-17}\exp\left(\frac{-9508}{T}\right) \qquad T < 1381$$

$$D_2 = 2.14\times10^{-13}\exp\left(\frac{-22884}{T}\right) \qquad 1381 \le T \le 1650 \qquad (33)$$

$$D_1 = 1.09\times10^{-17}\exp\left(\frac{-6614}{T}\right) \qquad T > 1650$$

The diffusion coefficients in Equation 33 were used in the Mathcad program, since they are the coefficients used by Forsberg and Massih and the basis for the coefficients used in FRAPCON-3. It appears that Equation 33 is an empirical fit to data and is taken to be representative of the diffusion of a single gas atom in UO_2, regardless of the type of gas atom. It would be necessary to obtain appropriate diffusion coefficients for an accurate calculation.

A slight modification was made to the temperature range over which coefficients D_1 and D_2 were used in the Forsberg and Massih model and the Booth model. Instead of basing the diffusion coefficient on a temperature range, it was based on the values of the expressions for D_1 and D_2 (Equation 33) that gave the lowest diffusion coefficient at the temperature in question. This was done to smooth out the transition from D_1 to D_2, similar to what is done in the FRAPCON-3 model. The effects were minor and only shifted the temperature range over which D_1 was applicable by a few degrees. The diffusion coefficients calculated from Equation 33 were used to calculate the fission gas release for the Forsberg and Massih model and the Booth model.

The diffusion coefficients used for FRAPCON-3 were calculated using the procedures described in the FRAPCON-3 literature [4, 14].. The high temperature diffusion coefficient, D_3, in Equation 33 was not used. The activation energy for D_2 was multiplied by 1.15, and the coefficient is multiplied by a burnup enhancement factor (Equation 34), when the burnup is high enough to give the factor a value greater than 1 [14]. The selection of the diffusion coefficient is based on the expression that gives the lowest value. After all other modifications have been preformed; the calculated diffusion coefficient is multiplied by 12, which is a fitting parameter.

$$100^{\frac{BURNUP-21}{35}}, \text{where BURNUP} = \text{burnup in } \frac{GWd}{MTU} \text{ [14]} \qquad (34)$$

While trying to implement the original Forsberg and Massih model, issues similar to those reported in the FRAPCON-3 literature were encountered. Issues related to the resolution term, $h_4\beta_e$ (Equations 20 and 21), and the treatment of the resolved gas were two of the main issues. These issues needed to be resolved before results could be obtained from the Forsberg and Massih model.

The resolution parameter is related to the probability of a bubble on the grain boundary undergoing resolution, b_{gb}, a distance, λ. Figure 4 shows how the release curves change as b_{gb} is changed by taking it to be equal to different percentages of b'. Taking 1% of b' gives a value for $b_{gb}\lambda$ of 9.7 x10^{-13}, that is about two orders of magnitude higher than the resolution parameter of 1.84 x10^{-14} suggested by Forsberg et. al. [16]. If a value of 9.7 x10^{-13} is used for the parameter $b_{gb}\lambda$, then the amount of gas resolved at the grain boundary is not physically reasonable. If a value of 1.84x10^{-14} is used the results are more reasonable. To get a value that is on the order of 1.84x10^{-14} would require either the probability of resolution to be about 0.01% of b' or the resolution depth to be roughly 10^{-10} m. A resolution depth of 10^{-10} m would not be physically reasonable. For consistency, and because there was no evidence to support the use of 1% b', a value of 1.84x 10^{-14} was used for the composite parameter $b_{gb}\lambda$ (or ~0.01% of b').

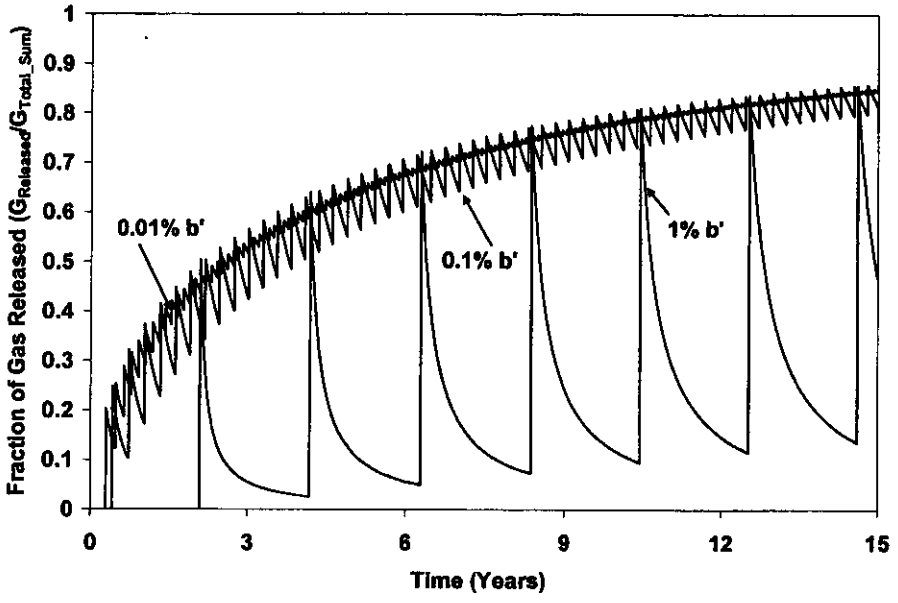

Figure 4 Differences in the gas release curves for different values of *b'* for the Forsberg and Massih model.

The y-axis in Figure 4 is the fraction of gas released to an external surface, obtained by dividing the gas released from the fuel by the sum of the gas at the grain boundary, in the grain, and released from the fuel (sum of gases). Another way to determine the fraction of gas released is to divide the amount of gas released by the total amount of gas produced *(βt)* (produced gas). Figure 5 shows a comparison between release curves obtained by dividing the amount of gas released by either the total amount of gas produced or the sum of the gases. It is apparent that large discrepancies exist between the curves. The release curves were calculated using two different values for the rate of resolution of an intergranular bubble, b_{gb}. It is apparent that as the b_{gb} decreases, which corresponds to less gas being resolved back into the grain boundary, the differences between the curves are less. This suggests that the discrepancies are related to the treatment of the resolved gas that has been identified as an issue with the Forsberg/Massih model in the FRAPCON-3 literature [14]. This was addressed in FRAPCON-3 by releasing both the gas at the grain boundary and the resolved gas when saturation is reached [14]. A similar approach was used in this study for results calculated using the gas produced.

Figure 6 shows the results for fraction of gas released calculated using the Booth, Forsberg/Massih, and FRAPCON-3 models. Results were obtained by using both the gas produced [Figure 6(b)] and the sum of the gas in the grain, on the grain boundary, and released from the fuel [Figure 6(a)]. The fraction of gas released from the fuel to an external surface calculated using the different models are in good agreement. The slightly higher amount of gas released in the FRAPCON-3 model is most likely due to the modified diffusion coefficient, which is slightly larger than that used in the other two models. The shapes of the curves and the time to release are different for each model.

The Forsberg/Massih and FRAPCON-3 models require that the concentration of the gas on the grain boundaries reaches a saturation value before it is released. At time of release it is assumed that an interconnected network of grain boundary bubbles is formed which allows the gas to escape. FRAPCON-3 assumes that once the gas is released, the concentration of gas at the grain boundaries goes to zero and the network of tunnels collapse. Further release of gas does not occur until saturation conditions are reached again. It was not explicitly stated by Forsberg and Massih [2] how the release of gas should be treated once saturation conditions were met. Therefore, for consistency, the formation of tunnels, release of gas from the fuel, and then collapse of the tunnels was used for the both the FRAPCON-3 and Forsberg/Massih models. This leads to the saw tooth shape of the Forsberg/Massih and FRAPCON-3 models. The time to each release is related to the amount of gas that is resolved from the grain boundary, which is proportional to $b_{gb}\lambda$ (Equation 20). These saw tooth release curves are consistent with what is shown in the FRAPCON-3 literature [14]. When the FRAPCON-3 model is applied to an entire fuel rod, which contain regions of different temperatures, the release curve tends to smooth out [14].

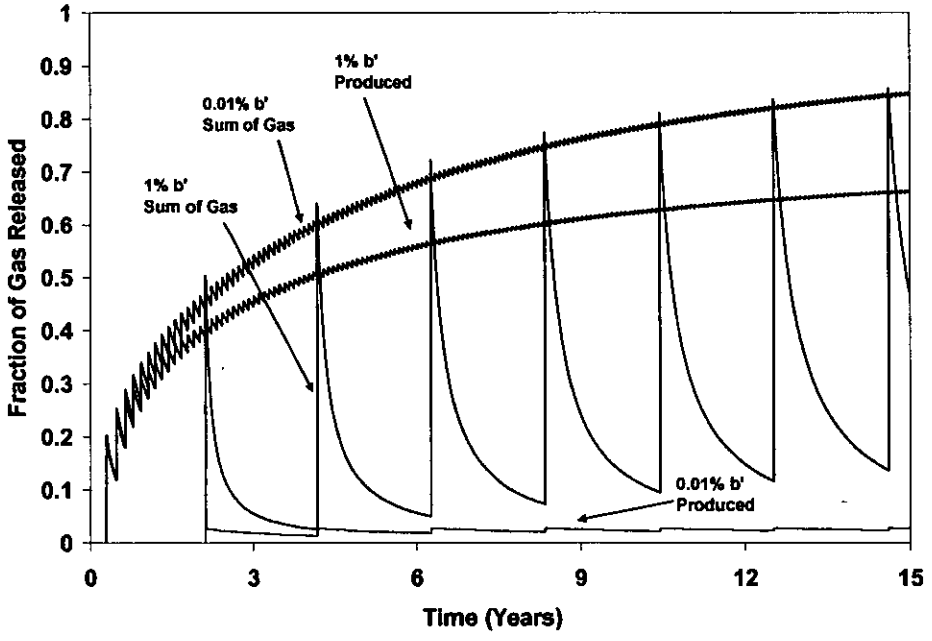

Figure 5 **Gas release curves for different values of b_{gb} and calculated using the produce gas and sum of the gases.**

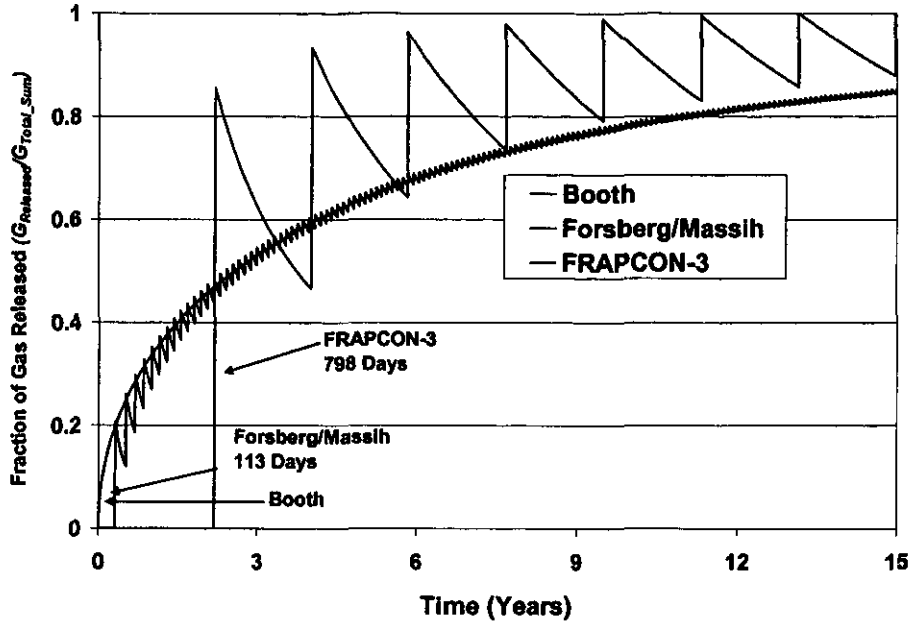

(a)

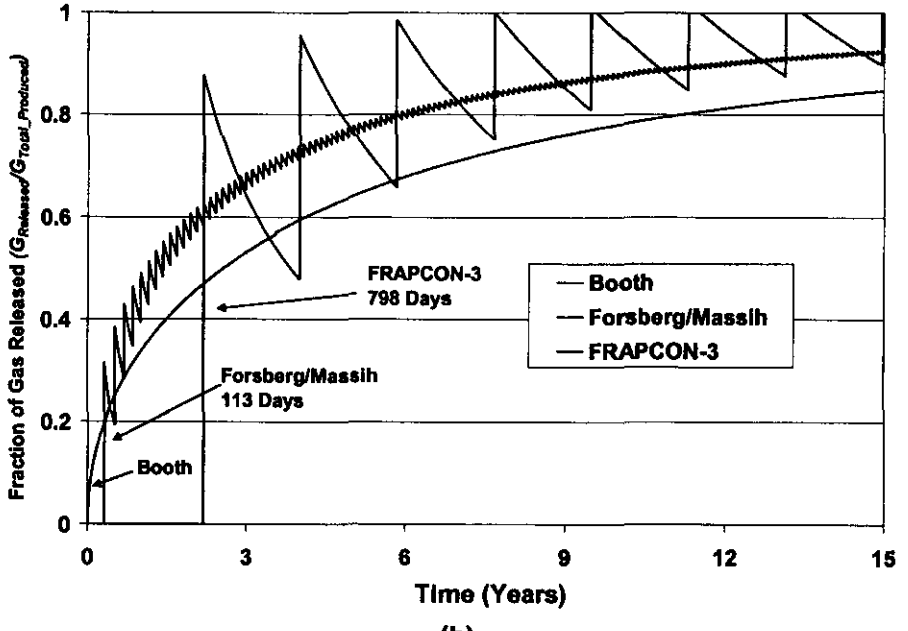

(b)

Figure 6 **Fraction of gas released calculated using the (a) sum of gas concentrations and (b) total amount of gas produced for UO_2 fuel with a grain radius of 10 μm held at 1650 K for 15 years.**

The longer time required for saturation conditions to be met and for the onset of gas release in the FRAPCON-3 model relative to the original Forsberg/Massih model is due to the larger amount of gas that is resolved during each time step in the FRAPCOn-3 model. Figure 7 shows the fraction of the gas that is resolved back into the 10 μm grain for a given time step, using the D_1 and D_2 from Equation 33 and the FRAPCON-3 modifications. As the temperature increases, the amount of gas resolved into the grain decreases, but even at 1800 K, about 90% of the gas arriving at the grain boundary is resolved back into the grain. For the conditions used in these calculations, 99% of the gas is resolved. The amount of gas resolved back into the grain for the Forsberg/Massih model is around 44% and therefore the time to reach grain boundary saturation is much less. The difference in amount of gas resolved for each model is related to the modified diffusion coefficient and the fit multiplier, *FITMULT*, (Equation 32) used in the FRAPCON-3 model. Because of the issues related to the Forsberg and Massih model the results will not be included for the remainder of this document. The discussion below demonstrates how the fission gas release predicted from the current FRAPCON-3 model is affected by changes in the grain size and temperature.

The grain size of the fuel will affect the total fraction of gas that is released at a given time. Figure 8 shows the fraction of gas released for different grain radii (calculated using the sum of the gases) as a function of time for the Booth and FRAPCON-3 models at 1650 K. As the grain size increases, the fission gases must diffuse a greater distance to reach the grain boundary, thereby reducing the fraction of gas released at a given time. In addition, the time until gas is release calculated using the FRAPCON-3 model increases as the grain size increases (Figure 9). There is competition between the increase in grain boundary area for small gains, which leads to higher gas concentrations at saturation (Figure 10), and the shorter distance that gas must diffuse to reach the grain boundary, which results in a shortened amount of time until release. The overall fraction of gas release that is predicted by the FRAPCON-3 model agrees well with the fraction of gas release predicted by the Booth model (Figure 8). The difference in agreement between the FRAPCON-3 and Booth curves in Figure 8 compared to Figure 6 is related to differences in the diffusion coefficients. In Figure 8 the diffusion coefficient used in both models has been modified using the procedures described in the FRAPCON-3 literature [4, 14]; whereas, in Figure 6 the diffusion coefficient used in the Booth model has not been modified .

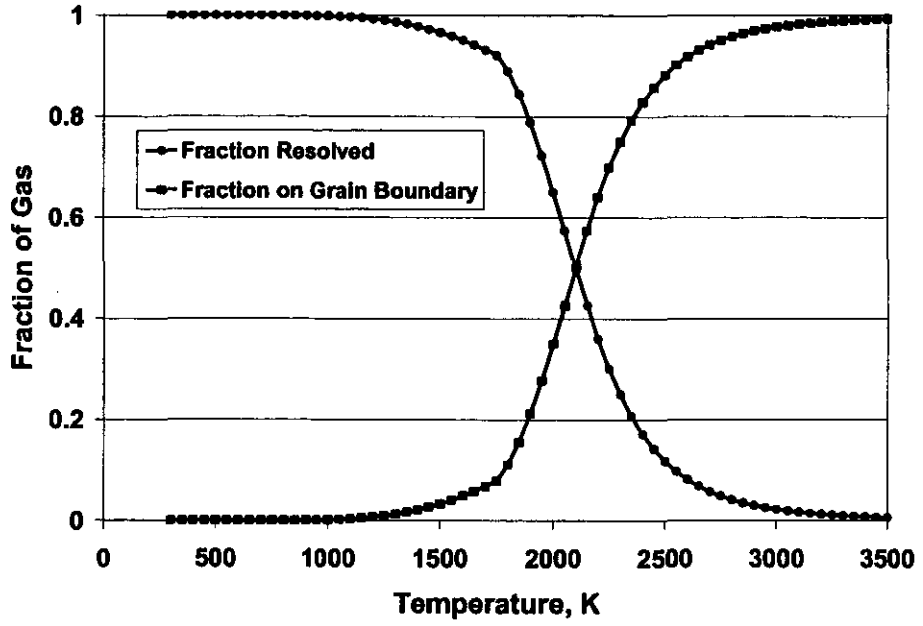

Figure 7 **The fraction of gas resolved and fraction of gas on the grain boundary as a function of temperature calculated using the FRAPCON-3 resolution parameter.**

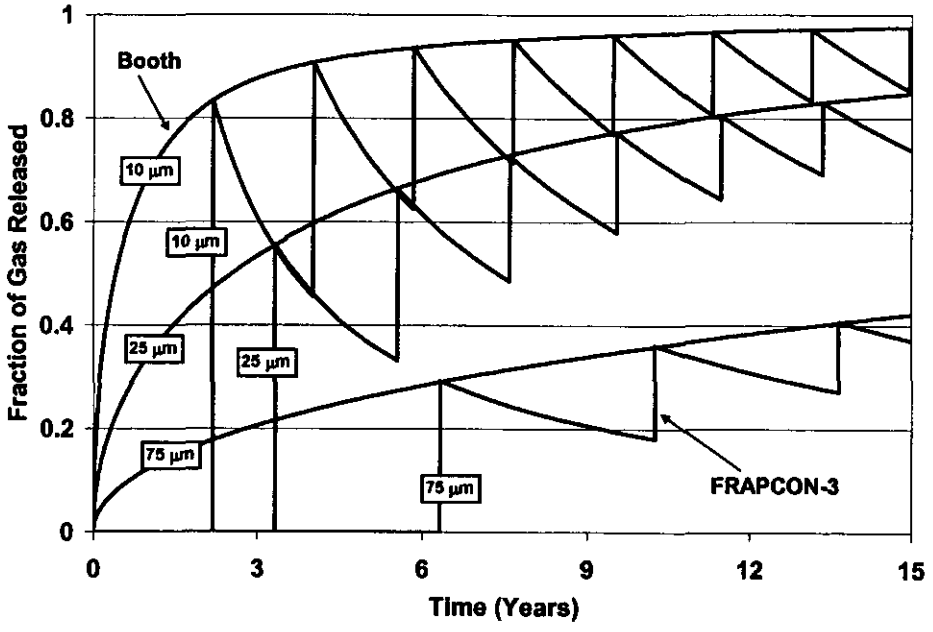

Figure 8 **Fraction of gas released as function of grain size calculated, using the Booth and FRAPCON-3 ($G_{released}/G_{Total\_Sum}$) models and a temperature of 1650 K.**

Changes in the temperature of the fuel will also affect the amount of gas that is released. Figure 11 shows the fraction of calculated gas release, using the Booth and FRAPCON-3 models, for a 10 μm grain radius at different temperatures as a function of time. As the temperature increases, the diffusion coefficient increases and, therefore, the time necessary for gas created in the grain to diffuse to the grain boundary decreases. This leads to a higher fraction of gas being released at higher temperatures. In addition, the time-to-release calculated using the FRAPCON-3 model decreases (Figure 12). Grain boundary growth, which could be significant at relatively high temperatures, is not taken into account in the current FRAPCON-3 model.

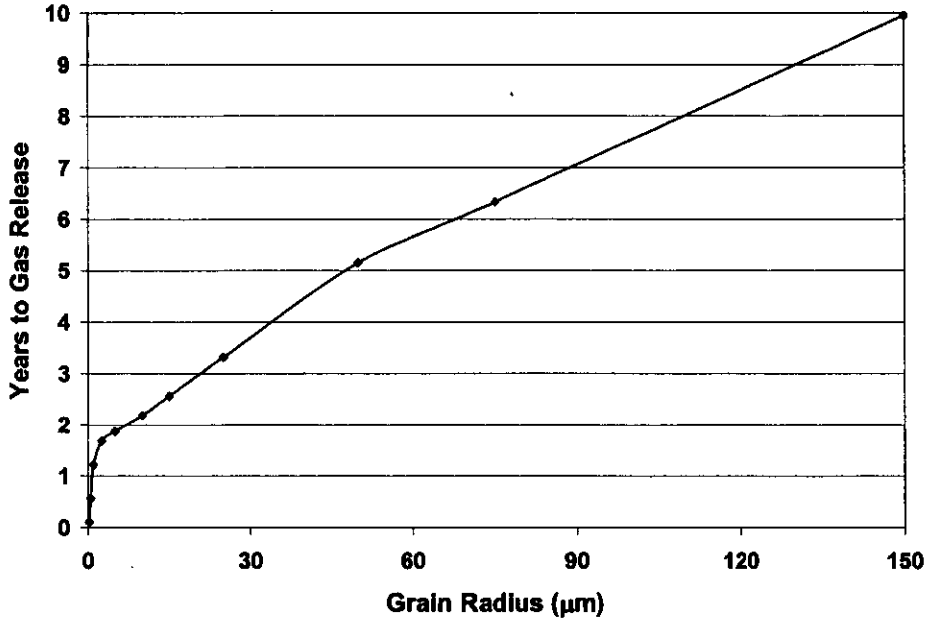

Figure 9 Number of years to gas release for different grain radii calculated using the FRAPCON-3 model and a temperature of 1650 K.

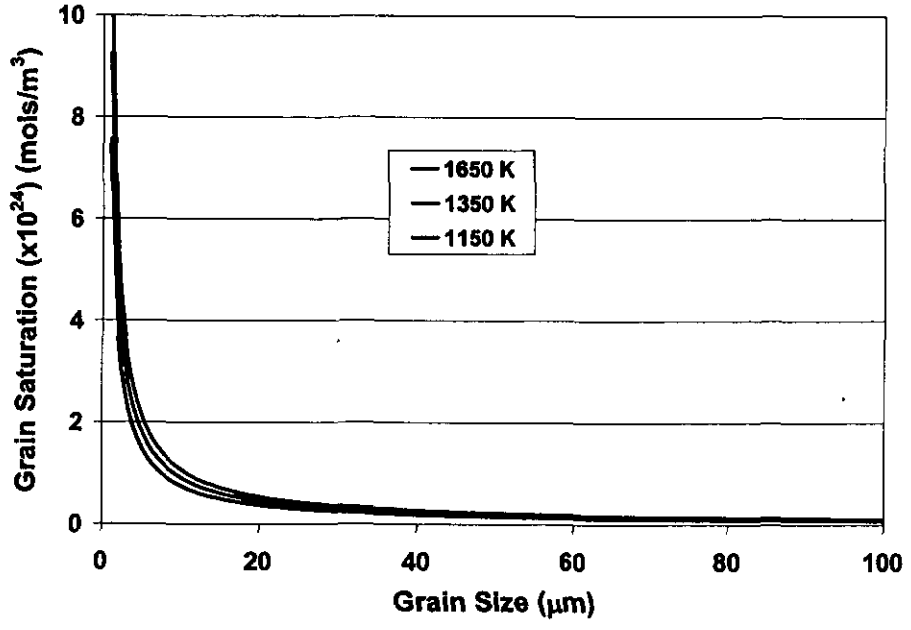

Figure 10 **Concentration of gas required for saturation as a function of grain size for different temperatures.**

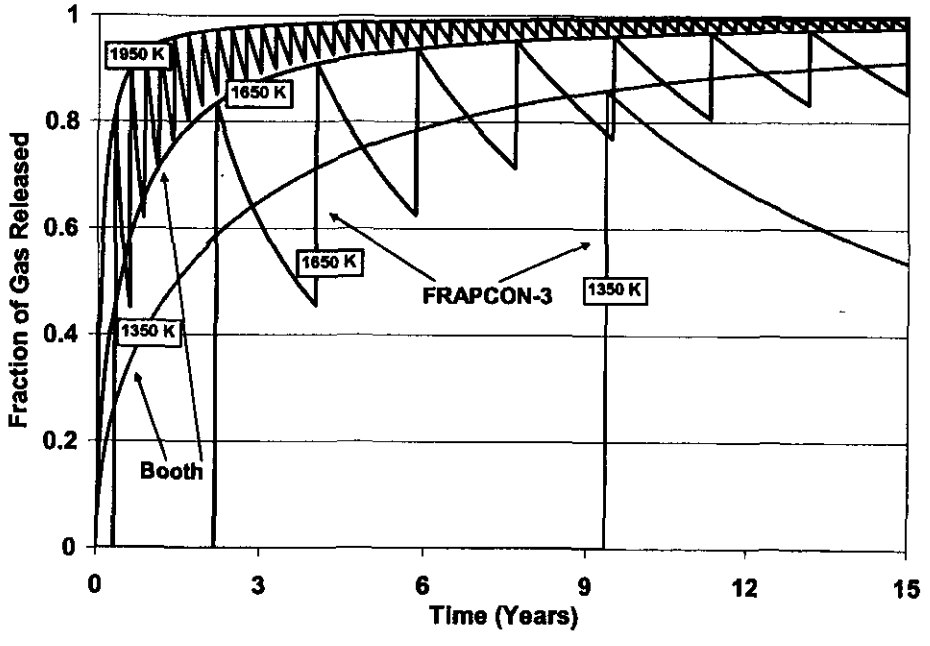

Figure 11 **Fraction of gas released as function of temperature calculated, using the Booth and FRAPCON-3 ($G_{released}/G_{Total\_Sum}$) models for a grain radius of 10μm.**

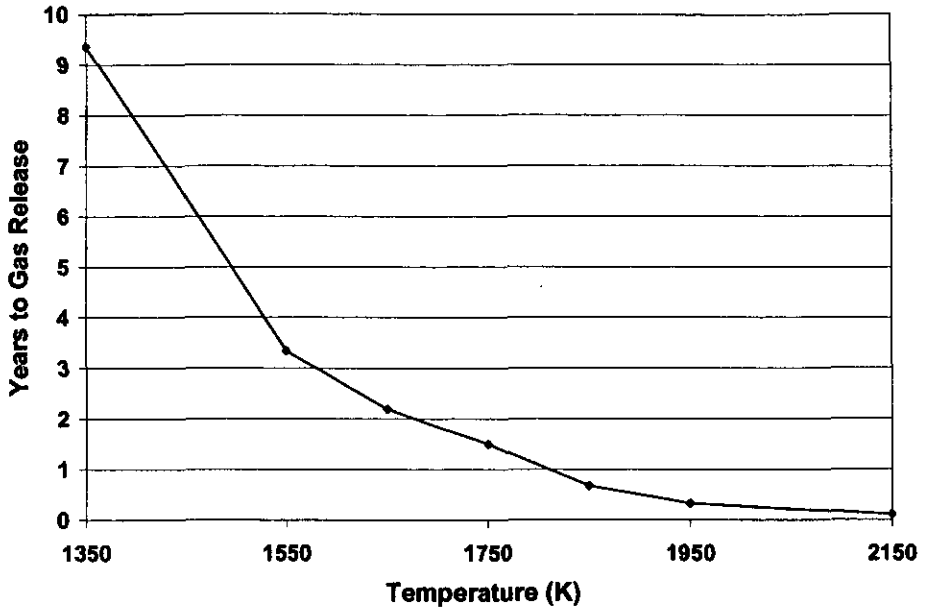

Figure 12 Number of years to gas release for different temperatures calculated using the FRAPCON-3 model and grain radius of 10 μm.

Conclusions:

It is important to have a good understanding of the amount of fission gas that will be released during reactor operation for proper design. Initially it was thought that the application of a two-stage fission gas release model may be more descriptive of the gas release phenomena. There is some evidence that gas release could be controlled by tailoring the grain size and fuel temperature. However, it has become clear at this time that both the Forsberg/Massih and FRAPCON-3 models cannot be used without further development. It is notable that, despite a generally similar methodology, the Forsberg/Massih and FRAPCON-3 techniques predict drastically different fission gas release behaviors. In both cases, it is apparent that the input parameters are not well understood and are often order-of-magnitude best estimates. In addition, there are some issues related to the resolution parameters used in the original Forsberg and Massih model and how to deal with the resolved gas. These issues have been overcome in the FRAPCON-3 model by forcing the results to fit physical data using multiplication factors. However, the data used to tune the FRAPCON-3 model was collected from specimens that experienced a much higher fission rate relative to what would be expected for the Prometheus mission. It would be necessary to validate the FRAPCON-3 model with data that is collected under more prototypical conditions if this model were to be used. At this time it seems most appropriate to use the over-simplified and conservative Booth model until a model that more accurately describes fission gas release can be developed.

Future Work

If the Prometheus project would not have been restructured, a decision needed to be made on whether to continue using the Booth model, attempt to verify the FRAPCON-3 model, or develop a new fission gas release model. Verification of the FRAPOCN-3 model or development of a new fission gas release model would require testing under Prometheus conditions and extensive development. The

benefits gained from a physically representative model would need to be weighed against the effort required to develop the model. At this time it is unclear as to whether or not a more complete understanding of the gas release in the early stages of reactor operation would be worth the effort required for the development.

Significance to the NR Program:

An improved understanding of time to and the amount of fission gas that is released into the fuel pin is beneficial for reactor design. The goal of this work was to gain an understanding of the Forsberg and Massih and FRAPCON-3 two-stage gas release models to determine if they could be applied to calculate fission gas release under Prometheus conditions. At this time it is apparent that neither model can be used to calculate fission gas release under Prometheus conditions.

Acknowledg-ments:

The author would like to acknowledge Dave Noe for his technical advice and mentoring during this work. In addition, the author would like to thank John Glass, Beth Lugert, James Volmer, John Beale, and Lynne Kolaya for their technical review of this letter.

Prepared by:

M. Krohn, Senior Engineer
Space Reactor Materials Engineering
MT-Advanced Materials Technology

Approved by:

R. Baranwal, Acting Manager
Space Reactor Materials Engineering
MT-Advanced Materials Technology

References:

1. Booth, A.H., *A Method of Calculating Fission Gas Diffusion From UO_2 Fuel and Its Application to the X-2-f Loop Test, AECL Report No. 496.* 1957.

2. Forsberg, K. and A.R. Massih, *Diffusion Theory of Fission Gas Migration in Irradiated Nuclear Fuel UO_2.* Journal of Nuclear Materials, 1985. **135.**

3. Mathsoft Engineering & Education, I., *Mathcad, version 11.0.* 2002.

4. Berna, G.A., et al., *FRAPCON-3: A Computer Code for the Calculation of Steady-State Thermal-Mechanical Behavior of Oxide Fuel Rods for High Burnup, Vol. 2 PNNL-11513.* 1997, Pacific Northwest National Laboratory.

5. Olander, D.R., *Fundamental Aspects of Nuclear Reactor Fuel Elements.* 1976, Division of Reactor Development and Demonstration, Energy Research and Development Administration: Berkeley.

6. MDO-723-0054, K.L., *Review of Restructuring of UO_2 for the Prometheus Reactor.* Nov. 2005.

7. Speight, M.V., *A Calculation of the Migration of Fission Gas in Material Exhibiting Precipitation and Re-solution of Gas Atoms Under Irradiation.* Nuclear Science and Engineering, 1969. **37**: p. 180-185.

8. Ham, F.S., *Theory of Diffusion -Limited Precipitation.* Journal of Physics and Chemistry of Solids, 1958. **6**: p. 335-351.

9. Baker, C., *The Fission Gas Bubble Distribution in Uranium Dioxide from High Temperature Irradiated SGHWR Fuel Pins.* Journal of Nuclear Materials, 1977. **66**: p. 283-291.

10. White, R.J. and M.O. Tucker, *A New Fission-Gas Release Model.* Journal of Nuclear Materials, 1983. **118**: p. 1-38.

11. Turnbull, J.A., *The Effect of Grain Size on the Swelling and Gas Release Properties of UO_2 During Irradiation.* Journal of Nuclear Materials, 1974. **50**: p. 62-68.

12. Dowling, D.M., R.J. White, and M.O. Tucker, *The Effect of Irradiation -Induced Re-Solution on Fission Gas Release.* Journal of Nuclear Materials, 1982. **110**: p. 37-46.

13. Reynolds, G.L., W.B. Beere, and P.T. Sawbridge, *The Effect of Fission Products on the Ratio of Grain-Boundary Energy to Surface Energy in Irradiated Uranium Dioxide.* Journal of Nuclear Materials, 1971. **41**: p. 112.

14. Lanning, D.D., C.E. Beyer, and C.L. Painter, *FRAPCON-3: Modifications to Fuel Rod Material Properties and Performance Models for High-Burnup Applications, Vol. 4 PNNL-11513.* 1997, Pacific Northwest National Laboratory.

15. Geelhood, K., *Personal Communication.* 2005, PNNL. p. Discussion about FRAPCON-3 approach to implement Forsberg and Massih.

16. Forsberg, K., F. Lindstrom, and A.R. Massih. *Modeling of Some High Burnup Phenomena in Nuclear Fuel, paper 2.5.* in *Technical Committee Meeting on Water Reactor Fuel Element Modeling at High Burnup , and Experimental Support.* 1994. Windermere, England, IWGFPT/41: International Atomic Energy Agency, Vienna, Austria.

17. Carrol, R.M., O. Sisman, and R.B. Perez, *The Effects of Fission Density on Fission-Gas Release.* Nuclear Science and Engineering, 1968. **32**: p. 430.

18. Carrol, R.M. and O. Sisman, *In-Pile Fission-Gas Release from Single Crystal UO_2.* Nuclear Science and Engineering, 1965. **21**: p. 147-158.

19. Turnbull, J.A., *A Review of Irradiation Induced Re-solution in Oxide Fuel.* Radiation Effects, 1980. **53**: p. 243.

20. Olander, D.R., *FRAPCON-3: Modifications to Fuel Elements.* 1997, Division of Reactor Development and Demonstration, Energy Research and Development Administration: Berkeley.

21. Nichols, F.A., *Transport Phenomena in Nuclear Fuels.* Journal of Nuclear Materials, 1979. **84**: p. 1-25.

22. Forsberg, K. and A.R. Massih. *Theory of Fission Gas Release During Grain Growth.* in *Transactions, SMiRT 16.* 2001.

23. Friskney, C.A. and J.A. Turnbull, *CEGB Report No. RD/B/N4217.* 1980.

24. Turnbull, J.A., et al., *CEGB Report No. RD/B/N4892.* 1980.

25. Turnbull, J.A. and C.A. Friskney, *The Relationship Between Microstructure and the Release of Unstable Fission Products During High Temperature Irradiation of Uranium Dioxide.* Journal of Nuclear Materials, 1978. **71**: p. 238.

This Page Intentionally Left Blank

Appendix 1
Mathcad Worksheet for Gas Release

Author: Matthew Krohn

Fission Gas Release Model- Forsberg/Massih, FRAPCON-3, and Booth

This Mathcad worksheet uses the equations derived by *K. Forsberg and A.R. Massih* (**Journal of Nuclear Materials 135 (1985) 140-148**) to calculate the fraction of fission gas release.

Forsberg and Massih considered the following equation:

$$\frac{d}{dt}C(r,t) := D(t)\left(\frac{d^2}{dr^2}C(r,t) + \frac{2}{r}\cdot\frac{d}{dr}C(r,t)\right) + \beta(t)$$

where

$C(r,t)$= Concentration which is a function of position and time, assumed to be generated uniformly thorough out a grain of radius a
$D(t)$= Time dependent diffusion coefficient
$\beta(t)$= Gas production Rate
r = radial distance

Subject to the following boundary conditions:

$$C(r,0) := 0$$

$$C(a,t) := \frac{\beta(t)\cdot\lambda\cdot N(t)}{2\cdot D(t)}$$

This approach takes into account grain boundary saturation. The gas concentration at the grain boundary needs to reach a saturation concentration before it is released. This model is set up so that once the gas is released the pathways close and the saturation conditions must be again for. This model does not take into account grain growth and grain boundary sweeping.

This program is set up with collapsible regions. Double click the arrow under the headings to expand the region. To collapse the regions double click the arrow at the bottom of the region.

User Input required for the fission rate calculations

This section allows the user to set the fission rate, which can be defined or calculated by Mathcad. The user can set whether the fission rate is calculated using fissions per initial fissile atoms (FIFA) or fissions per initial metal atoms (FIMA)

Calculated or User Defined Fission Rate $Cal\_Fission := 1$

Set **Cal_Fission** equal to **1** to have the Mathcad calculate the fission rate.
Set **Cal_Fission** equal to **0** to use the user defined fission rate.

Enter user defined fission rate: $F_{User} := 1.5\times 10^{18}$ (Fissions/sec*m^3)

****Cal_Fission** must be equal to **0** for user defined fission rate to be used in the calculations ******

FIFA or FIMA Fission Rate Calculations

Set **Cal_Type** equal to **1** for a **FIFA** calculation.
Set **Cal_Type** equal to **0** for a **FIMA** calculation. $Cal\_Type := 1$

*****Cal_Fission** must be equal to **1** for calculated fission rate to be used in the calculations ******

Physical Constants and Materials Parameters

Enter grain radius of UO_2 fuel $a_o := 10 \times 10^{-6}$ (Initial grain radius, m)

This region contains physical constants that are used for the calculations. They were taken from the literature. References for these values can be found in letter B-MT(SRME)-56.

Double click arrow to expand or collapse section.

(average fission fragment length, m)
$l_f := 6 \cdot 10^{-6}$

(fission fragment range of influence, m)
$Z_o := 10^{-9}$

(Resolution depth, m)
$\lambda := 10^{-8}$

(Avogadro's Number, atoms/mole)
$N_A := 6.022 10^{23}$

(Boltzman's Constant, J/K)
$k_b := 1.38 10^{-23}$

(Free surface energy for UO_2 from Olander, J/m^2)
$\gamma := 0.6$

(Grain boundary bubble radius, m)
$r_{gb} := 0.5 \cdot 10^{-6}$

(Fraction of gas released when grain boundary saturation is reached)
$f_R := 1.0$

(Applied external pressure, Pa)
$P_{ext} := 0$

Fuel Characteristics

This region contains user defined variables related to fuel that are used to calculate fission rate.

Double click arrow to expand or collapse section.

(Enrichment)
$E := 0.93$

(Burn Up, fraction)
$BU := 0.03$

(Theoretical Density Natural UO_2 Fuel, g/cc)
$\rho_{UR} := 10.98$

(Volume fraction of porosity)
$P_{Vol} := 0.03$

(Fraction of gas produced)
$F_{Gas} := 0.30$

(Energy per fission, MeV)
$E_{MeV} := 188$

Time and Temperature Inputs

This region allows the user to input the time and temperature. Time is divided into a set number of evenly spaced time steps based on the users input. Currently the program is set to allow for one temperature change, but could easily be modified to account from multiple temperature changes.

Enter temperature and time parameters

(Total time in years) (Time step, days) (Starting temp, K) (Ending temp, K)

$t_{Total} := 15$ $\Delta t_{days} := 1$ $T_S := 1650$ $T_1 := 1650$

(Time at starting temp, days) (Time during temperature change, days)

$t_1 := 365$ $t_{change} := 50$

Double click arrow to expand or collapse section.

Time Steps

(Time step, seconds)

$\Delta t := \Delta t_{days} \cdot 24 \cdot 3600$ $\Delta t = 86400$

(Number of steps)

$$i_{end} := \left[round\left[\frac{\left(t_{Total} \cdot 365 \cdot 24 \cdot 3600\right)}{\Delta t_{days} \cdot 24 \cdot 3600} \right] \right] - 1 \qquad i_{end} = 5474$$

$i := 0 .. i_{end}$

(Time, seconds)

$t_{(i+1)} := \Delta t \cdot (i + 1)$

$t_0 := 0$

Temperature Profile

(Change in temp, K)

$\Delta T_1 := T_1 - T_S$ $t_2 := t_{change} + t_1$

(Time at final temp, days)

$t_{end} := t_{i_{end}}$

(Temperature Profile, ^{O}K)

$$T(t) := \begin{cases} T_S \text{ if } 0 \le \frac{t}{86400} \le t_1 \\ \left[T_S + \left[\Delta T_1 \cdot \left[\frac{\left(\frac{t}{86400} \right) - t_1}{t_2 - t_1} \right] \right] \right] \text{ if } t_1 < \frac{t}{86400} \le t_2 \\ T_1 \text{ if } t_2 < \frac{t}{86400} \le t_{end} \end{cases}$$

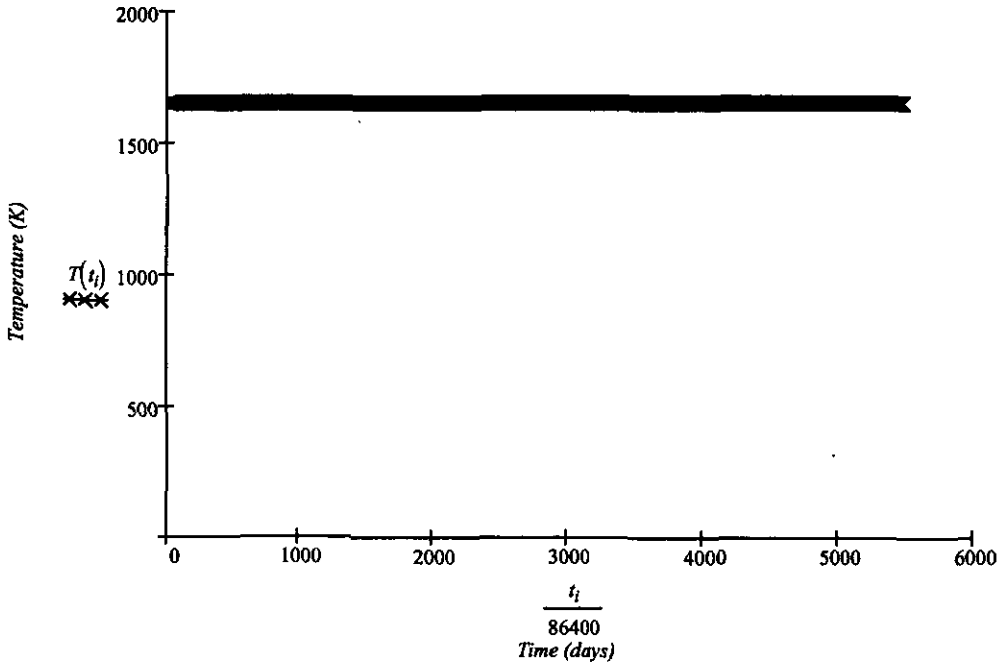

Fission Rate Calculations

This region contains the equations that calculate the fission rate based on the fuel characteristics and the time entered by the user. The user can set how the fission rate is calculated (FIFA or FIMA). In additions the user can set a user defined fission rate to be used in the calculations.

Double click arrow to expand or collapse section.

(Values defined by the user above)

$$NU := \begin{cases} E & \text{if } Cal\_Type = 1 \\ 1 & \text{if } Cal\_Type = 0 \end{cases} \qquad CalcType := \begin{cases} \text{"FIFA"} & \text{if } Cal\_Type = 1 \\ \text{"FIMA"} & \text{if } Cal\_Type = 0 \end{cases}$$

Density Enriched UO_2 Fuel, g/cc)

$$\rho_E := \left[(1-E)\cdot\rho_{UR}\right] + \left[E\cdot\rho_{UR}\left[\left(\frac{235.043923062}{238.029}\cdot\frac{238.029}{238.029+31.9988}\right) + \frac{31.9988}{238.029+31.9988}\right]\right]$$

$\rho_E = 10.867$

(Molecular Weight of Enriched UO_2 Fuel, g/mole)

$$MW_E := [(1-E)\cdot 270.0278 + E\cdot 235.043923062] + 31.998$$

$MW_E = 269.492$

(Moles of U_{235} or U cc of enriched UO_2, FIMA)

$$Moles_{U235} := NU\cdot\frac{1}{MW_E}\cdot\rho_E\cdot\left(1-P_{Vol}\right) \qquad Moles_{U235} = 3.638\times 10^{-2}$$

(Atoms of U_{235} per cc of enriched UO_2)

$$A_{U235} := Moles_{U235} \cdot N_A$$

$$A_{U235} = 2.191 \times 10^{22}$$

(Fission Rate, Fissions/sec*m^3)

$$F_{Calc} := \frac{A_{U235} \cdot BU}{t_{Total} \cdot 365 \cdot 24 \cdot 3600} \cdot \frac{1 \cdot 10^6}{1}$$

(Values defined by the user above)

$$F := \begin{cases} F_{Calc} & \text{if } Cal\_Fission = 1 \\ F_{User} & \text{if } Cal\_Fission = 0 \end{cases} \qquad FissionType := \begin{cases} \text{"Caclulated"} & \text{if } Cal\_Fission = 1 \\ \text{"User Defined"} & \text{if } Cal\_Fission = 0 \end{cases}$$

Fission Rates

Calculated

$F_{Calc} = 1.389 \times 10^{18}$ (Fissions/sec*m^3) $CalcType$ = "FIFA"

User Defined

$F_{User} = 1.5 \times 10^{18}$ (Fissions/sec*m^3)

Fission Rate Used in Calculations

$FissionType$ = "Caclulated" $F = 1.389 \times 10^{18}$ (Fissions/sec*m^3)

Model Parameters

This region contains the equations used to calculate the parameters necessary for the fission gas release models.
Double click arrow to expand or collapse section.

(Burnup, GWd/MTU is used to calculate the burnup enhancement factor (BEF) that is used in the FRAPCON-3 model to modify the diffusion coefficients

$$BURNUP(t) := F \cdot \frac{E_{MeV}}{1} \cdot \frac{1 \cdot 10^6}{1} \cdot \frac{1.602 10^{-19}}{1} \cdot \frac{1}{1 \cdot 10^6} \cdot \frac{t}{86400} \cdot \frac{1}{1 \cdot 10^6} \cdot \frac{1}{\rho_E} \cdot \frac{1000}{1}$$

$$BEF(t) := \begin{cases} 1 & \text{if } 100^{\frac{BURNUP(t)-21}{35}} \le 1 \\ 100^{\frac{BURNUP(t)-21}{35}} & \text{otherwise} \end{cases}$$

(Fission gas production rate)

$$\beta_{(i+1)} := F \cdot F_{Gas} \qquad \beta_{(0)} := F \cdot F_{Gas}$$

(Diffusion coefficient data taken from Forsberg and Massih, J. Nucl. Mater. 135 (1985) 140-148 derived from White and Tucker, J. Nucl. Mater. 118 (1983) 1-38, m^2/s)

(Low Temperature Diffusion Coefficient)

$$D_1(t) := 1.51 \cdot 10^{-17} \cdot exp\left(\frac{-9508}{T(t)}\right)$$

(Midrange Temperature Diffusion Coefficient)

$$D_2(t) := 2.14 \cdot 10^{-13} \cdot exp\left(\frac{-22884}{T(t)}\right)$$

(High Temperature Diffusion Coefficient)

$$D_3(t) := 1.09 \cdot 10^{-17} \cdot exp\left(\frac{-6614}{T(t)}\right)$$

Modified diffusion coefficients used in the FRAPCON-3 model- The modifications are as follows:

$$D_{1F}(t) := 12 \cdot 1.51 \cdot 10^{-17} \cdot exp\left(\frac{-9508}{T(t)}\right) \qquad D_{2F}(t) := 12 \cdot BEF(t) \cdot 2.14 \cdot 10^{-13} \cdot exp\left(\frac{-22884 \cdot 1.15}{T(t)}\right)$$

$$D_{int}(t) := \begin{cases} D_1(t) \text{ if } \begin{cases} T(t) \le 1381 \\ D_1(t) > D_2(t) \end{cases} \\ D_2(t) \text{ if } D_1(t) \le D_2(t) \le D_3(t) \\ D_3(t) \text{ otherwise} \end{cases}$$

$$D_{intF}(t) := \begin{cases} D_{1F}(t) \text{ if } D_{1F}(t) > D_{2F}(t) \\ D_{2F}(t) \text{ otherwise} \end{cases}$$

(Total gas bubble density, derived from Baker's data Baker, J. Nucl. Mater. 66 (1977) 283.)

$$C_b(t) := \frac{9.98 \cdot 10^{26}}{T(t)} - 1.42 \cdot 10^{23}$$

(Mean bubble radius, derived from Baker's data Baker, J. Nucl. Mater. 66 (1977) 283.)

$$r_b(t) := 1.806 \cdot 10^{-9} \cdot exp\left(1.039 \cdot 10^{-3} \cdot T(t)\right) + 4.591 \cdot 10^{-11}$$

(Capture rate at bubbles, given by Ham, Ham, J. Phys. Chem. Solids 6 (1958) 335.)

$$g(t) := 4 \cdot \pi D_{int}(t) \cdot r_b(t) \cdot C_b(t)$$

(Resolution probability from grain face intragranular bubbles, taken from White and Tucker, J. Nucl. Mater. 118 (1983) 1-38 derived from Baker's data Baker, J. Nucl. Mater. 66 (1977) 283.)

$$b(t) := 3.03 \cdot F \cdot \pi \cdot l_f \left(r_b(t) + Z_o\right)^2$$

(Effective diffusion coefficient, which takes into account resolution and capture of diffusing atoms by gas bubbles, Speight, Nucl. Sci. and Eng. 37 (1969) 180.)

Forsberg/Massih

$$D_{eff}(t) := D_{int}(t) \cdot \frac{b(t)}{b(t) + g(t)}$$

FRAPCON-3

$$D_{effF}(t) := D_{intF}(t)$$

FRAPCON-3 model tuned to data, does not explicitly deal with trapping

Grain Boundary Saturation

This region contains the equations used to calculate grain boundary saturation. This value is compared to the grain boundary gas concentration to determine if gas is released in a given time step.

Double click arrow to expand or collapse section.

$\theta := 50 \cdot deg$ (Accepted dihedral angle for intergranular bubbles in UO_2 from Reynolds, Beere, and Sawbridge, J. Nucl. Mater. 41 (1971) 112.)

$f(\theta) := 1 - \frac{3 \cdot \cos(\theta)}{2} + \frac{(\cos(\theta))^3}{2}$ (Shape factor, White and Tucker, J. Nucl. Mater. 118 (1983) 1-38)

$$f(\theta) = 1.686 \times 10^{-1}$$

$V_c := 0.25$ (Fractional coverage of grain boundary at saturation taken from White and Tucker, J. Nucl. Mater. 118 (1983) 1-38)

$N_{s_i} := \left[\frac{4 \cdot r_{gb} \cdot f(\theta) \cdot V_c}{3 \cdot k_b \cdot T(t_i) \cdot (\sin(\theta))^2} \cdot \left(\frac{2 \cdot \gamma}{r_{gb}} + P_{ext} \right) \right]$ (Density of state equation from Dowling White and Tucker, J. Nucl. Mater. 110 (198) 37, assumes ideal gas equation used to calculate density of gas particles over whole grain boundary at saturation.)

$G_{s_i} := \frac{3}{2 \cdot a_o} \cdot N_{s_i}$ (Density of gas within the grain boundaries at saturation, moles/m^3)

Scaled Time, τ (integration of effective diffusion coefficient over time)

This region contains the integrals for calculating the scale time parameter, τ.

Double click arrow to expand or collapse section.

Forsberg/Massih

$\Delta\tau_{i+1} := \int_{t_i}^{t_{i+1}} D_{eff}(t)\, dt$ $\tau_{i+1} := \left(\sum_{o=0}^{i+1} \Delta\tau_o \right)$

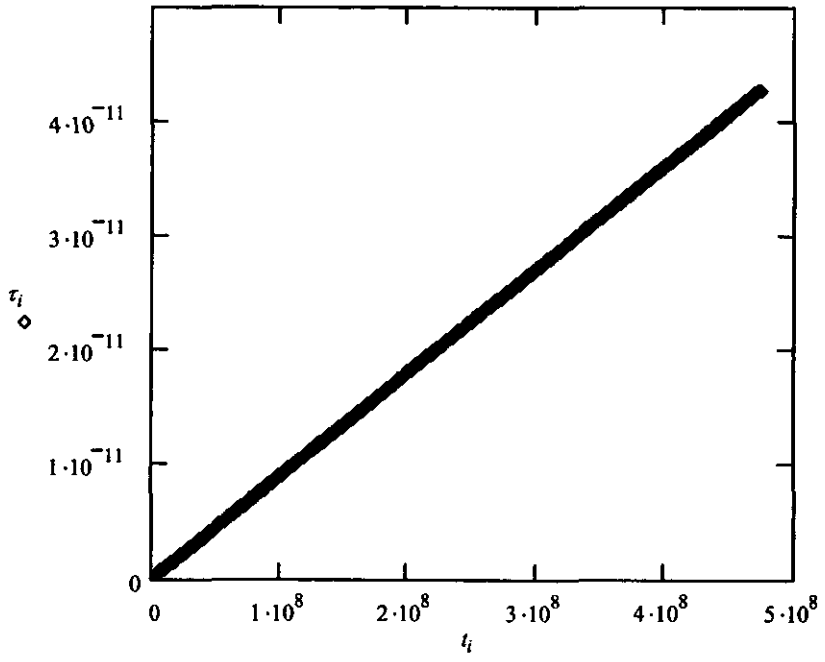

FRAPCON-3

$$\Delta\tau F_{i+1} := \int_{t_i}^{t_{i+1}} D_{effF}(t)\,dt \qquad \tau F_{i+1} := \left(\sum_{o=0}^{i+1} \Delta\tau F_o \right)$$

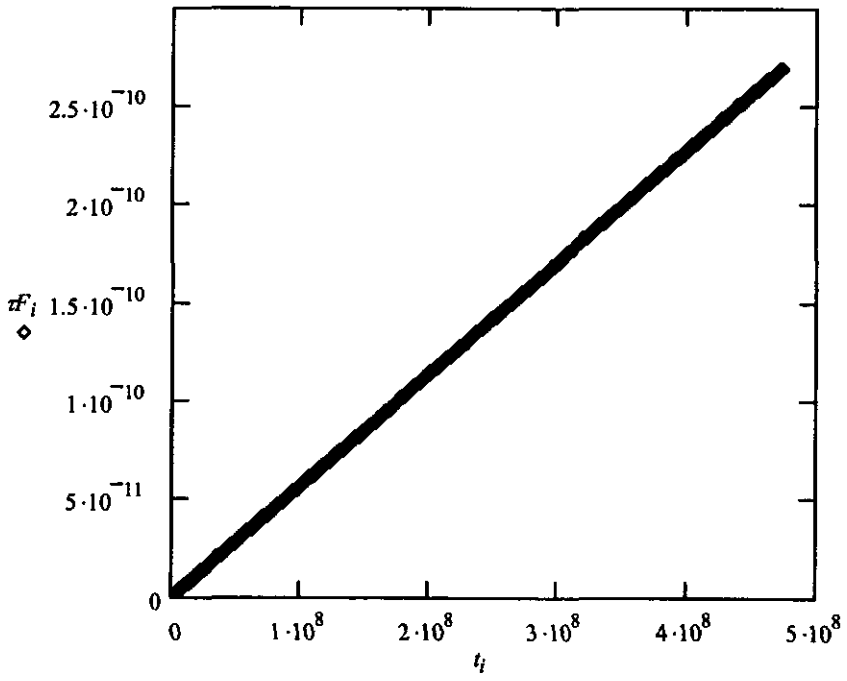

Booth equations for gas release

This region contains the short and long time approximations for the Booth model.

Double click arrow to expand or collapse section.

Approximation of Booth Model Taken from AECL Report 496 (CRDC-721)

$$\omega_i := \frac{D_{eff}(t_i)\cdot t_i}{a_o^{\,2}}$$

(Fraction of gas released calculated using the Booth Model approximations)

$$f_{c_i} := \begin{cases} 4\cdot\left(\frac{\omega_i}{\pi}\right)^{\frac{1}{2}} - \frac{3}{2}\cdot\omega_i & \text{if } \omega_i \le \pi^{-2} \\ \frac{0.57}{\pi^2\cdot\omega_i} + 1 - \frac{1}{\pi^2\cdot\omega_i} - \frac{6\cdot e^{-1}}{\pi^4\cdot\omega_i} + \frac{6\cdot e^{-\pi^2\cdot\omega_i}}{\pi^4\cdot\omega_i} & \text{if } \omega_i > \pi^{-2} \end{cases}$$

Approximations to kernel K_3 taken from Forsberg and Massih

Double click arrow to expand or collapse section.

(Approximation of $1+K_3(t)$ from Forsberg and Massih, J. Nucl. Mater. 135 (1985) 140-148)

$$n := 1..3 \quad A_n := \begin{cases} 0.63003 & \text{if } n = 1 \\ 0.20651 & \text{if } n = 2 \\ 0.14776 & \text{if } n = 3 \end{cases} \qquad B_n := \begin{cases} 9.9904 & \text{if } n = 1 \\ 64.488 & \text{if } n = 2 \\ 511.61 & \text{if } n = 3 \end{cases}$$

Forsberg and Massih equations taken from FRAPCON-3

This region contains the FRAPCON-3 equations for calculating gas release.

The FRAPCON code uses optimization parameters to modify the equations derived by Forsberg and Massih. These parameters are factors which affect the diffusion coefficients and the resolution effects. The modifications are as follows:

1.) **Diffusion coefficient are multiplied by 12**
2.) **D_2 is multiplied by a burnup enhancement factor.**
    The equations can be found in the model parameters section.
3.) **The activation term for D_2 is multiplied by 1.15**
4.) **The resolution term is multiplied by 300.**
5.) **D_3 is not used**

Double click arrow to expand or collapse section.

$$f_{1F_0} := 0 \qquad f_{2F_0} := 0$$

$$f_{1F_{i+1}} := \left[exp\left[\frac{-B_1 \cdot \left(\pi F_{i+1} - \pi F_i \right)}{a_o^{\,2}} \right] \right] - 1 \qquad f_{2F_{i+1}} := \left[exp\left[\frac{-B_2 \cdot \left(\pi F_{i+1} - \pi F_i \right)}{a_o^{\,2}} \right] \right] - 1$$

$$f_{3F_0} := 0$$

$$f_{3F_{i+1}} := \left[exp\left[\frac{-B_3 \cdot \left(\pi F_{i+1} - \pi F_i \right)}{a_o^{\,2}} \right] \right] - 1$$

$$f\Delta\pi F_{i+1} := \begin{cases} \displaystyle\int_{\pi F_i}^{\pi F_{i+1}} \left[\frac{6}{\sqrt{\pi}} \cdot \left(\frac{\pi F_{i+1} - x}{a_o^{\,2}} \right)^{\frac{1}{2}} + 3 \cdot \left(\frac{\pi F_{i+1} - x}{a_o^{\,2}} \right) \right] dx \quad if \quad \pi F_{i+1} \le 0.1 \\ \displaystyle\int_{\pi F_i}^{\pi F_{i+1}} \left[1 - \left(\frac{6}{\pi^2} \right) \cdot exp\left[-\pi^2 \cdot \left(\frac{\pi F_{i+1} - x}{a_o^{\,2}} \right) \right] \right] dx \quad if \quad \pi F_{i+1} > 0.1 \end{cases}$$

(Initial Values)

$$G_{b_0} := 0 \qquad G_{o_0} := 0 \qquad G_{Total_0} := 0 \qquad f\Delta\pi F_0 := 0 \qquad G_{R_0} := 0$$

$$q_1 := \frac{\beta_1 \cdot \left(t_1 - t_0 \right)}{a_o^{\,2} \cdot \left[-\left(\frac{f_{1F_1} \cdot A_1}{B_1} + \frac{f_{2F_1} \cdot A_2}{B_2} + \frac{f_{3F_1} \cdot A_3}{B_3} \right) + f\Delta\pi F_1 \right]}$$

(Resolution Effect)

$$FitMult := 300$$

$$RE(t) := FitMult \cdot \left(\frac{1.84 \cdot 10^{-14} \cdot a_o}{3 \cdot D_{effF}(t)} \right)$$

$$\begin{bmatrix} q_{(i+1)} \\ G_{b_{(i+1)}} \\ G_{res_{i+1}} \\ G_{1_{(i+1)}} \\ G_{2_{(i+1)}} \\ G_{3_{(i+1)}} \\ G_{R_{(i+1)}} \\ t_{R_{i+1}} \end{bmatrix} := \begin{bmatrix} \dfrac{\beta_{i+1}\cdot\left(t_{i+1}-t_i\right)}{a_o^{\,2}\cdot\left[-\left(\dfrac{f_{1F_{i+1}}\cdot A_1}{B_1}+\dfrac{f_{2F_{i+1}}\cdot A_2}{B_2}+\dfrac{f_{3F_{i+1}}\cdot A_3}{B_3}\right)+f\Delta tF_{i+1}\right]} \\ \begin{cases} \left[G_{b_i}+\dfrac{\left[-\left(f_{1F_i}\cdot G1_i+f_{2F_i}\cdot G2_i+f_{3F_i}\cdot G3_i\right)+q_{i+1}\cdot f\Delta tF_{i+1}\right]}{1+RE\left(t_{i+1}\right)}\right] & \text{if } \dfrac{G_{b_i}}{G_{s_i}}<1 \\ \dfrac{\left[-\left(f_{1F_i}\cdot G1_i+f_{2F_i}\cdot G2_i+f_{3F_i}\cdot G3_i\right)+q_{i+1}\cdot f\Delta tF_{i+1}\right]}{1+RE\left(t_{i+1}\right)} & \text{if } \dfrac{G_{b_i}}{G_{s_i}}\geq 1 \end{cases} \\ \begin{cases} G_{res_i}+\dfrac{RE\left(t_{i+1}\right)}{1+RE\left(t_{i+1}\right)}\cdot\left[-\left(f_{1F_i}\cdot G1_i+f_{2F_i}\cdot G2_i+f_{3F_i}\cdot G3_i\right)+q_{i+1}\cdot f\Delta tF_{i+1}\right] & \text{if } \dfrac{G_{b_i}}{G_{s_i}}<1 \\ \dfrac{RE\left(t_{i+1}\right)}{1+RE\left(t_{i+1}\right)}\cdot\left[-\left(f_{1F_i}\cdot G1_i+f_{2F_i}\cdot G2_i+f_{3F_i}\cdot G3_i\right)+q_{i+1}\cdot f\Delta tF_{i+1}\right] & \text{if } \dfrac{G_{b_i}}{G_{s_i}}\geq 1 \end{cases} \\ G1_i+\left[\left(f_{1F_i}\cdot G1_i\right)+\left[A_1\cdot q_{i+1}\cdot\int_{tF_i}^{tF_{i+1}} exp\left[\dfrac{-B_1}{a_o^{\,2}}\cdot\left(tF_{i+1}-x\right)\right]dx\right]\right] \\ G2_i+\left[\left(f_{2F_i}\cdot G2_i\right)+\left[A_2\cdot q_{i+1}\cdot\int_{tF_i}^{tF_{i+1}} exp\left[\dfrac{-B_2}{a_o^{\,2}}\cdot\left(tF_{i+1}-x\right)\right]dx\right]\right] \\ G3_i+\left[\left(f_{3F_i}\cdot G3_i\right)+\left[A_3\cdot q_{i+1}\cdot\int_{tF_i}^{tF_{i+1}} exp\left[\dfrac{-B_3}{a_o^{\,2}}\cdot\left(tF_{i+1}-x\right)\right]dx\right]\right] \\ \begin{cases} G_{R_i} & \text{if } \dfrac{G_{b_i}}{G_{s_i}}<1 \\ G_{R_i}+G_{b_i}+G_{res_i} & \text{if } \dfrac{G_{b_i}}{G_{s_i}}\geq 1 \end{cases} \\ \begin{cases} t_{R_i}+\dfrac{\Delta t}{86400} & \text{if } G_{R_i}=0 \\ t_{R_i}+0 & \text{otherwise} \end{cases} \end{bmatrix}$$

$G_{o_{i+1}} := G_{1_{i+1}} + G_{2_{i+1}} + G_{3_{i+1}}$ (Density of gas within the unit volume of fuel, atoms/m^3)

$G_{grain_{i+1}} := G_{o_{i+1}} + G_{res_{i+1}}$

$G_{Total_{i+1}} := G_{grain_{i+1}} + G_{b_{i+1}} + G_{R_{i+1}}$

$$t_{ReleaseF3} := \begin{cases} \text{"No Gas Released"} & \text{if } t_{Ri_{end}} = \dfrac{t_{i_{end}}}{86400} \\ num2str\left(t_{Ri_{end}}\right) & \text{otherwise} \end{cases}$$

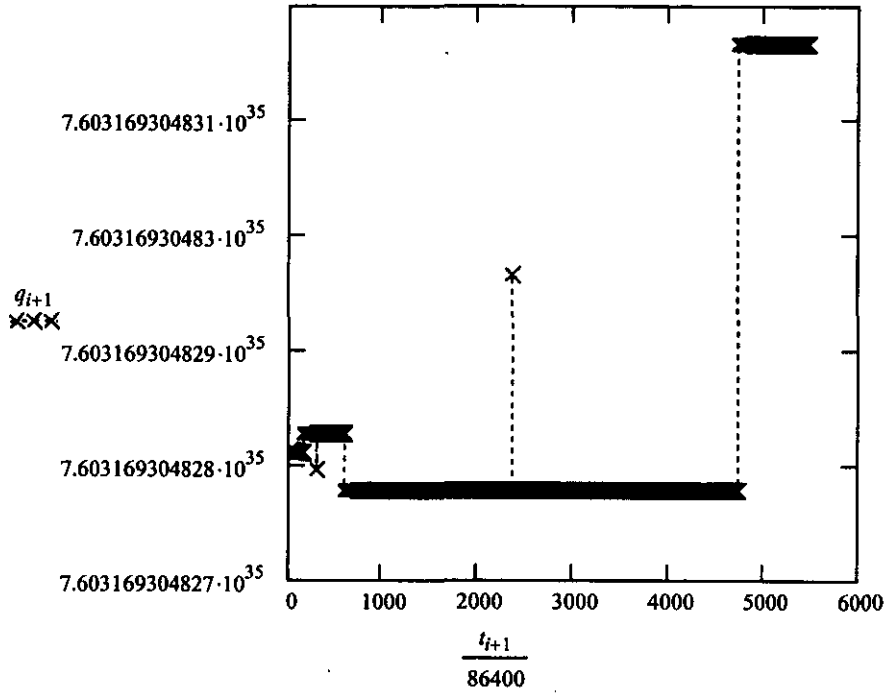

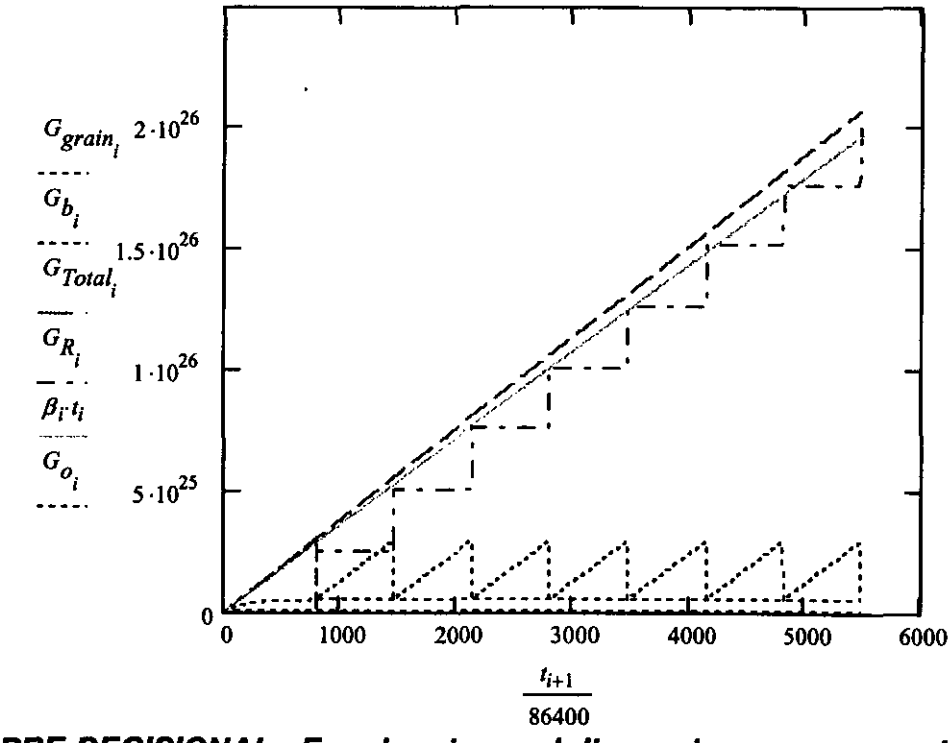

Result Check $x := 73$

$$\frac{t_x}{86400} = 7.3\times 10^{1}$$

$$G_{b_x} - G_{b_{x-1}} = 6.195\times 10^{20} \qquad G_{b_{x+1}} - G_{b_x} = 6.226\times 10^{20} \qquad G_{b_{x+2}} - G_{b_{x+1}} = 6.258\times 10^{20}$$

$$G_{res_x} - G_{res_{x-1}} = 2.001\times 10^{22} \qquad G_{res_{x+1}} - G_{res_x} = 2.011\times 10^{22} \qquad G_{res_{x+2}} - G_{res_{x+1}} = 2.021\times 10^{22}$$

$$G_{b_x} = 3.243\times 10^{22} \qquad G_{b_{x+1}} = 3.306\times 10^{22} \qquad G_{b_{x+2}} = 3.368\times 10^{22}$$

$$\frac{G_{b_x}}{G_{s_x}} = 4.284\times 10^{-2} \qquad \frac{G_{b_{x+1}}}{G_{s_{x+1}}} = 4.366\times 10^{-2} \qquad \frac{G_{b_{x+2}}}{G_{s_{x+2}}} = 4.449\times 10^{-2}$$

$$G_{res_x} = 1.048\times 10^{24} \qquad G_{res_{x+1}} = 1.068\times 10^{24} \qquad G_{res_{x+2}} = 1.088\times 10^{24}$$

$$G_{R_x} = 0\times 10^{0} \qquad G_{R_{x+1}} = 0\times 10^{0} \qquad G_{R_{x+2}} = 0\times 10^{0}$$

$$G_{grain_x} = 2.735\times 10^{24} \qquad G_{grain_{x+1}} = 2.772\times 10^{24} \qquad G_{grain_{x+2}} = 2.81\times 10^{24}$$

$$G_{Total_x} = 2.767\times 10^{24} \qquad G_{Total_{x+1}} = 2.805\times 10^{24} \qquad G_{Total_{x+2}} = 2.843\times 10^{24}$$

$$\beta_x \cdot t_x = 2.629\times 10^{24} \qquad \beta_{x+1} \cdot t_{x+1} = 2.665\times 10^{24} \qquad \beta_{x+2} \cdot t_{x+2} = 2.701\times 10^{24}$$

Forsberg and Massih equations

This region contains the Forsberg and Massih equations for calculating gas release.

Double click arrow to expand or collapse section.

$$f1_0 := 0 \qquad f2_0 := 0$$

$$f1_{i+1} := \left[exp\left[\frac{-B_1 \cdot (\tau_{i+1} - \tau_i)}{a_o^{\,2}} \right] \right] - 1 \qquad f2_{i+1} := \left[exp\left[\frac{-B_2 \cdot (\tau_{i+1} - \tau_i)}{a_o^{\,2}} \right] \right] - 1$$

$$f3_0 := 0 \qquad f3_{i+1} := \left[exp\left[\frac{-B_3 \cdot (\tau_{i+1} - \tau_i)}{a_o^{\,2}} \right] \right] - 1$$

$$f\Delta\tau_{i+1} := \begin{cases} \displaystyle\int_{\tau_i}^{\tau_{i+1}} \left[\frac{6}{\sqrt{\pi}} \cdot \left(\frac{\tau_{i+1} - x}{a_o^{\,2}} \right)^{\frac{1}{2}} + 3 \cdot \left(\frac{\tau_{i+1} - x}{a_o^{\,2}} \right) \right] dx & \text{if } \tau_{i+1} \le 0.1 \\ \displaystyle\int_{\tau_i}^{\tau_{i+1}} \left[1 - \left(\frac{6}{\pi^2} \right) \cdot exp\left[-\pi^2 \cdot \left(\frac{\tau_{i+1} - x}{a_o^{\,2}} \right) \right] \right] dx & \text{if } \tau_{i+1} > 0.1 \end{cases}$$

(Initial Values)

$$G2b_0 := 0 \qquad G2o_0 := 0$$

$$G2grain_0 := 0 \qquad G2Total_0 := 0$$

$$q2_1 := \frac{\beta_1 \cdot (t_1 - t_0)}{a_o^{\,2} \cdot \left[-\left(\frac{f1_1 \cdot A_1}{B_1} + \frac{f2_1 \cdot A_2}{B_2} + \frac{f3_1 \cdot A_3}{B_3} \right) + f\Delta\eta \right]}$$

(Resolution Effect)

$$h_0 := \frac{a_o \cdot 1.84\,10^{-14}}{3 \cdot \beta_{(1)}} \qquad \beta e_0 := \frac{\beta_1}{Deff(t_1)}$$

$$h_{(i+1)} := \frac{a_o \cdot 1.84\,10^{-14}}{3 \cdot \beta_{(i+1)}} \qquad \beta e_{(i+1)} := \frac{\beta_{(i+1)}}{Deff(t_{i+1})}$$

$$\begin{bmatrix} q2_{(i+1)} \\ G2b_{(i+1)} \\ G2I_{(i+1)} \\ G2Z_{(i+1)} \\ G2S_{(i+1)} \\ G2R_{(i+1)} \\ G2R2_{(i+1)} \\ t2R_{i+1} \end{bmatrix} := \left[\begin{array}{l} \dfrac{\beta_{i+1}\cdot\left(t_{i+1}-t_i\right)-h_{i+1}\cdot G2b_i\cdot\left(\beta e_{i+1}-\beta e_i\right)+h_{i+1}\cdot\beta e_{i+1}\cdot\left(f1_i\cdot G2I_i+f2_i\cdot G2Z_i+f3_i\cdot G2S_i\right)}{a_o^{\,2}\cdot\left[-\left(\dfrac{f1_{i+1}\cdot A_1}{B_1}+\dfrac{f2_{i+1}\cdot A_2}{B_2}+\dfrac{f3_{i+1}\cdot A_3}{B_3}\right)+\left(1+h_{i+1}\cdot\beta e_{i+1}\right)\cdot f\Delta\tau_{i+1}\right]} \\ \left| \begin{array}{ll} G2b_i+\left[-\left(f1_i\cdot G2I_i+f2_i\cdot G2Z_i+f3_i\cdot G2S_i\right)+f\Delta\tau_{i+1}\cdot q2_{i+1}\right] & \text{if } \dfrac{G2b_i}{Gs_i}<1 \\ -\left(f1_i\cdot G2I_i+f2_i\cdot G2Z_i+f3_i\cdot G2S_i\right)+f\Delta\tau_{i+1}\cdot q2_{i+1} & \text{if } \dfrac{G2b_i}{Gs_i}\geq 1 \end{array} \right. \\ G2I_i+\left[\left(f1_i\cdot G2I_i\right)+\left[A_1\cdot q2_{i+1}\cdot\displaystyle\int_{\tau_i}^{\tau_{i+1}}\exp\left[\frac{-B_1}{a_o^{\,2}}\cdot\left(\tau_{i+1}-x\right)\right]dx\right]\right] \\ G2Z_i+\left[\left(f2_i\cdot G2Z_i\right)+\left[A_2\cdot q2_{i+1}\cdot\displaystyle\int_{\tau_i}^{\tau_{i+1}}\exp\left[\frac{-B_2}{a_o^{\,2}}\cdot\left(\tau_{i+1}-x\right)\right]dx\right]\right] \\ G2S_i+\left[\left(f3_i\cdot G2S_i\right)+\left[A_3\cdot q2_{i+1}\cdot\displaystyle\int_{\tau_i}^{\tau_{i+1}}\exp\left[\frac{-B_3}{a_o^{\,2}}\cdot\left(\tau_{i+1}-x\right)\right]dx\right]\right] \\ \left| \begin{array}{ll} G2R_i+G2b_i & \text{if } \dfrac{G2b_i}{Gs_i}\geq 1 \\ G2R_i & \text{if } \dfrac{G2b_i}{Gs_i}<1 \end{array} \right. \\ \left| \begin{array}{ll} G2R2_i+G2b_i+h_i\cdot\beta e_i\cdot\left(G2b_i\right) & \text{if } \dfrac{G2b_i}{Gs_i}\geq 1 \\ G2R2_i & \text{if } \dfrac{G2b_i}{Gs_i}<1 \end{array} \right. \\ \left| \begin{array}{ll} t2R_i+\dfrac{\Delta t}{86400} & \text{if } G2R_i=0 \\ t2R_i+0 & \text{otherwise} \end{array} \right. \end{array} \right]$$

$$t_{ReleaseFM} := \left| \begin{array}{ll} \text{"No Gas Released"} & \text{if } t2R_{i_{end}}=\dfrac{t_{i_{end}}}{86400} \\ num2str\left(t2R_{i_{end}}\right) & \text{otherwise} \end{array} \right.$$

$$G2o_{i+1} := G2l_{i+1} + G2z_{i+1} + G2s_{i+1}$$

$$G2o2_{i+1} := G2l_{i+1} + G2z_{i+1} + G2s_{i+1}$$

$$G2grain_{i+1} := G2o_{i+1}$$

$$G2grain2_{i+1} := G2o_{i+1} + h_{i+1} \cdot \beta e_{i+1} \cdot \left(G2b_{i+1}\right)$$

$$G2Total_{i+1} := G2grain_{i+1} + G2b_{i+1} + G2R_{i+1}$$

$$G2Total2_{i+1} := G2grain_{i+1} + G2b_{i+1} + G2R2_{i+1}$$

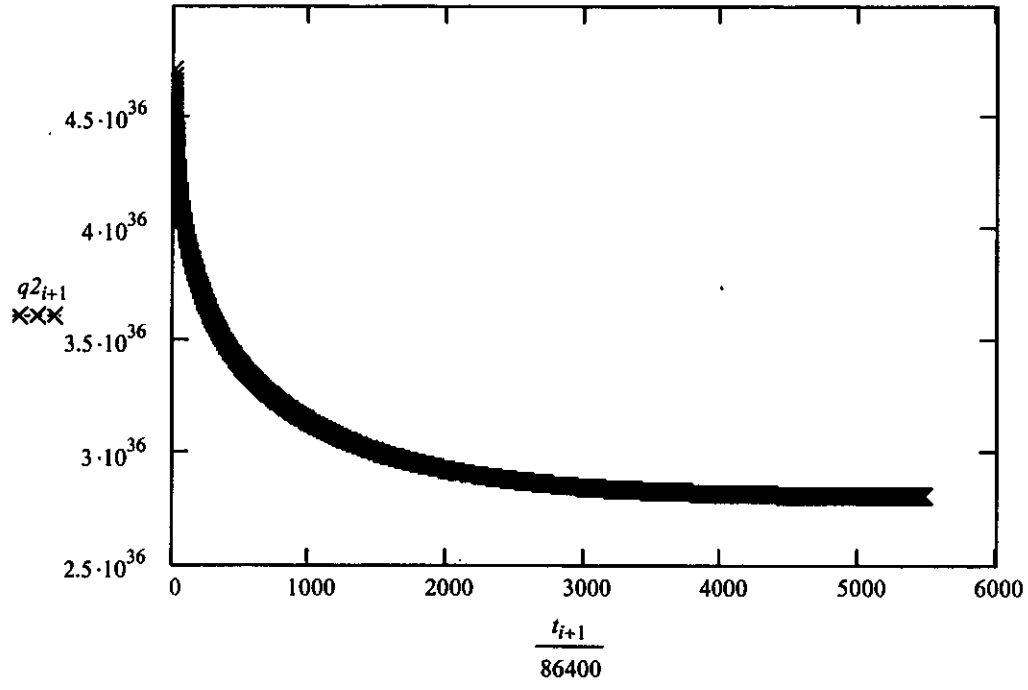

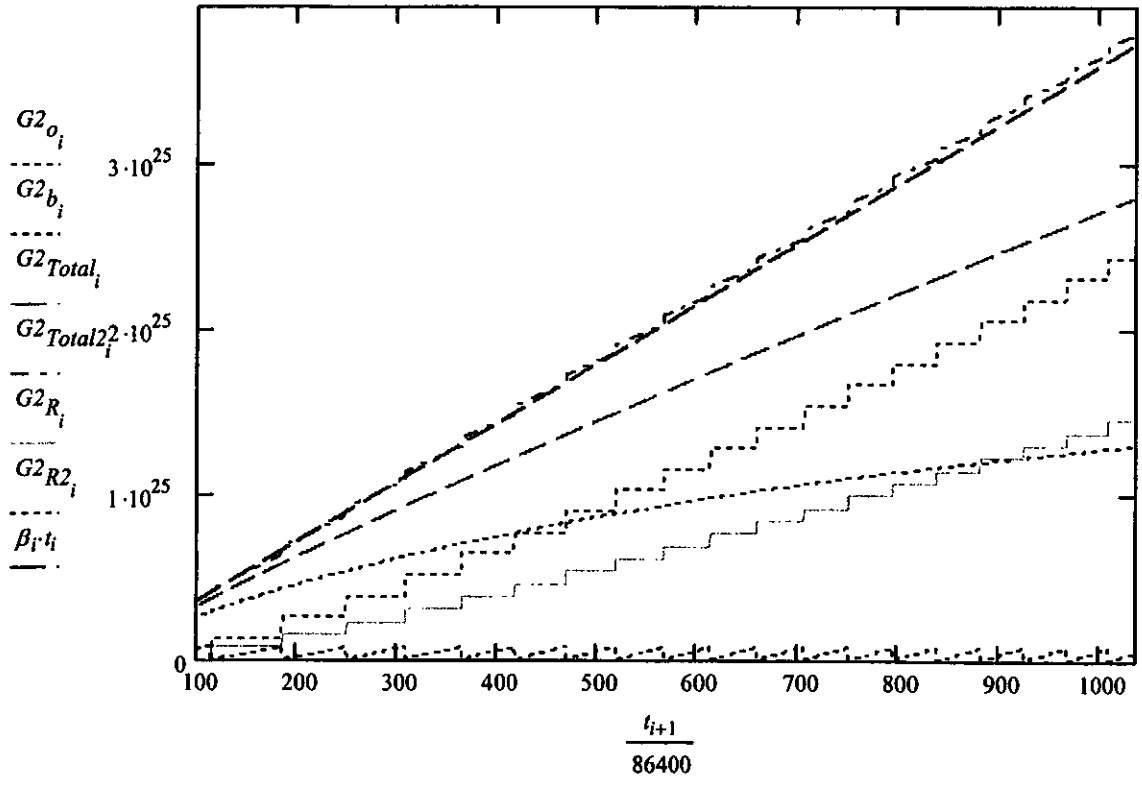

Result Check

$x := 765$

$$\frac{t_x}{86400} = 7.65\times 10^{2}$$

$$G2b_x - G2b_{x-1} = 1.72\times 10^{22} \qquad G2b_{x+1} - G2b_x = 1.721\times 10^{22} \qquad G2b_{x+2} - G2b_{x+1} = 1.721\times 10^{22}$$

$$G2b_x = 2.746\times 10^{23} \qquad G2b_{x+1} = 2.918\times 10^{23} \qquad G2b_{x+2} = 3.09\times 10^{23}$$

$$\frac{G2b_x}{G_{s_x}} = 3.627\times 10^{-1} \qquad \frac{G2b_{x+1}}{G_{s_{x+1}}} = 3.854\times 10^{-1} \qquad \frac{G2b_{x+2}}{G_{s_{x+2}}} = 4.081\times 10^{-1}$$

$$G2R_x = 9.934\times 10^{24} \qquad G2R_{x+1} = 9.934\times 10^{24} \qquad G2R_{x+2} = 9.934\times 10^{24}$$

$$G2grain_x = 1.112\times 10^{25} \qquad G2grain_{x+1} = 1.113\times 10^{25} \qquad G2grain_{x+2} = 1.114\times 10^{25}$$

$$G2Total_x = 2.133\times 10^{25} \qquad G2Total_{x+1} = 2.136\times 10^{25} \qquad G2Total_{x+2} = 2.138\times 10^{25}$$

$$\beta_x \cdot t_x = 2.755\times 10^{25} \qquad \beta_{x+1} \cdot t_{x+1} = 2.758\times 10^{25} \qquad \beta_{x+2} \cdot t_{x+2} = 2.762\times 10^{25}$$

Graphs

This region contains graphs of the calculated results

Double click arrow to expand or collapse section.

Number of Days until Gas Release

$t_{ReleaseF3} = "798"$

$t_{ReleaseFM} = "113"$

Number of Moles of Gas released per m^3

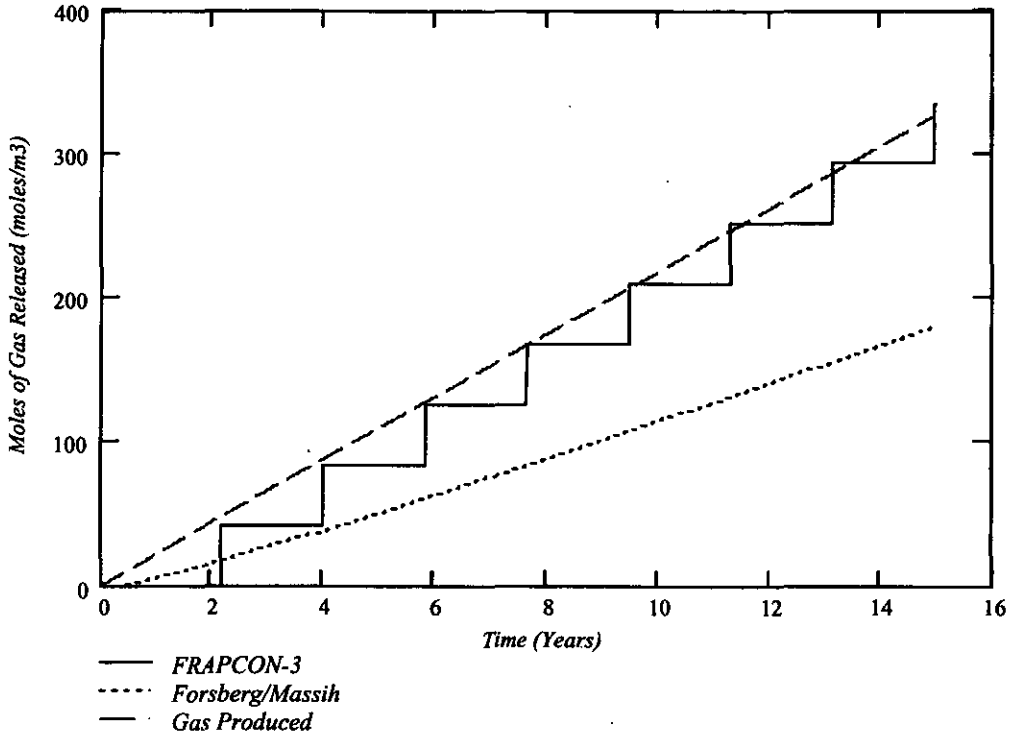

Fraction of Grain Boundary Saturation

(Gas concentration at grain boundary divided by grain boundary saturation gas concentration)

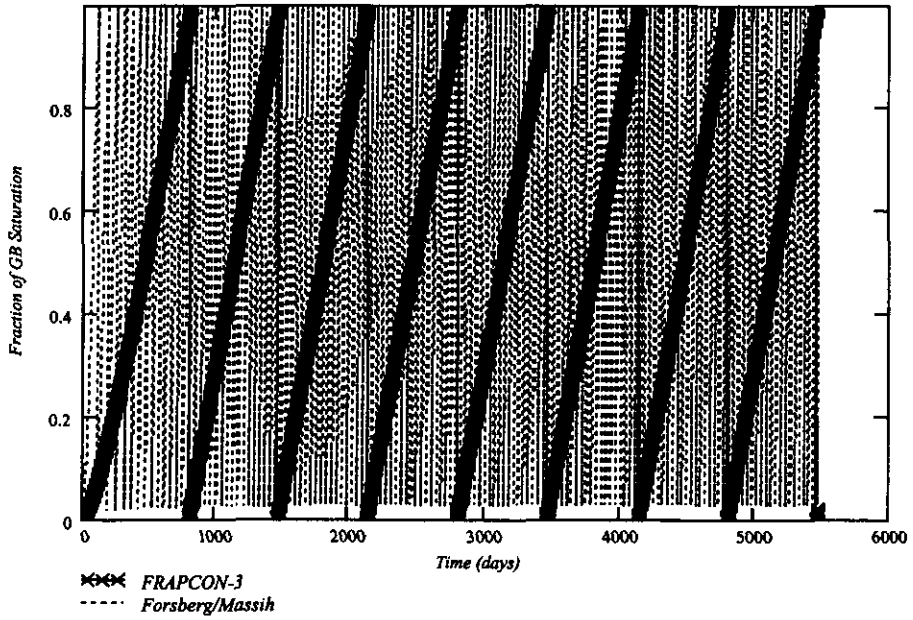

Fraction of gas released

(Gas released divided by total gas produced, which was calculated from production rate multiplied by time)

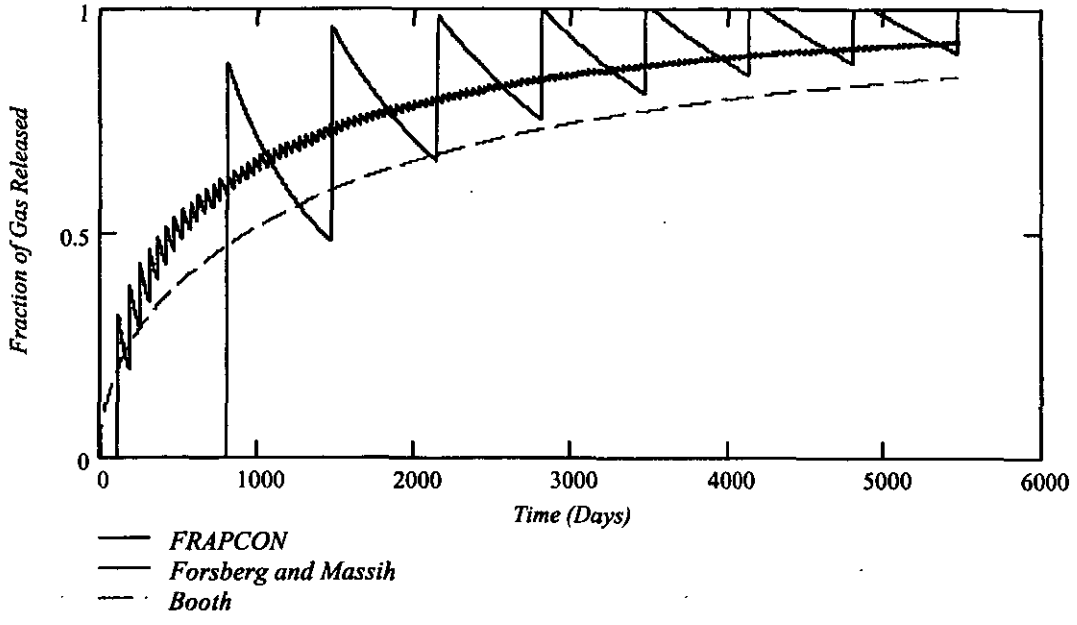

Fraction of gas released

(Gas released divided by total gas produced, which is calculated from the sum of the gas concentrations in the grain, on the grain boundary, and released)

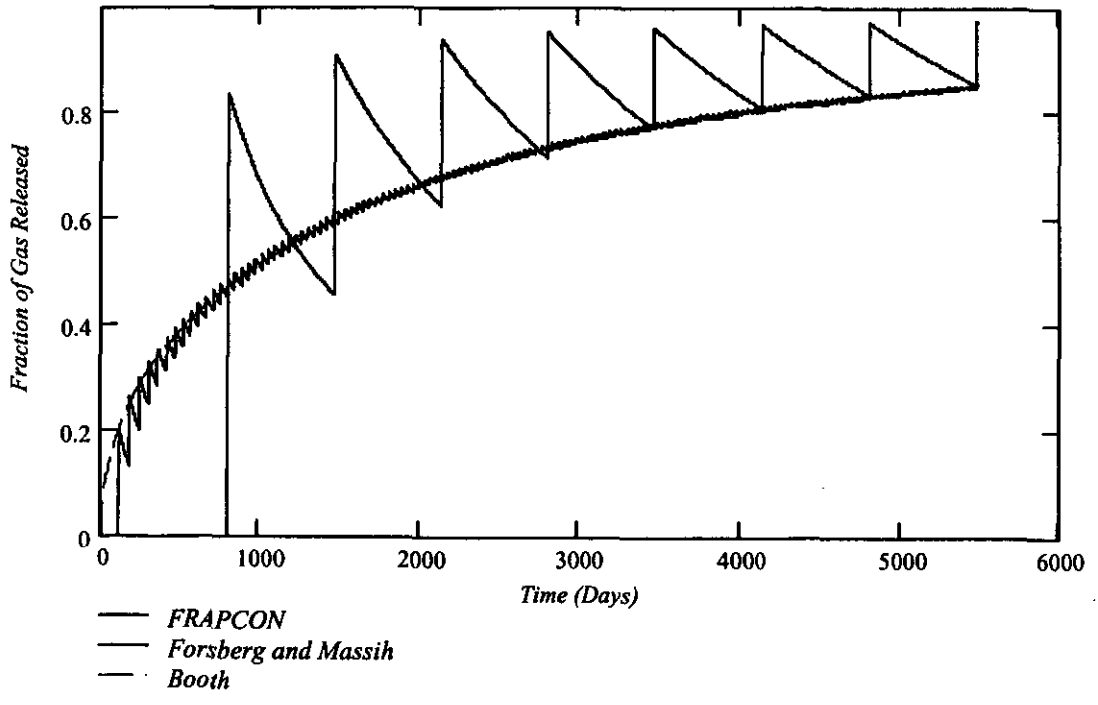

Data Output Matrix

This region contains a data matrix that can be output to data file, which can be opened in MS Excel.

Double click arrow to expand or collapse section.

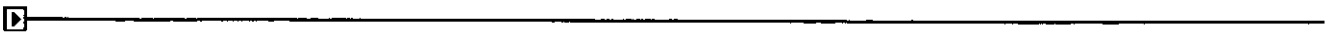

This Page Intentionally Left Blank

FORM 76082
4/1999

CONCURRENCE RECORD SHEET

- DOCUMENT NUMBER: B-MT(SRME)-56
- THIS DOCUMENT CONTAINS INFORMATION WHICH SHOULD BE CONSIDERED FOR PATENT DISCLOSURES ☐ YES ☒ NO
- THIS DOCUMENT CONTAINS INFORMATION WHICH MEETS BETTIS WORK CATEGORIES [A,B,C,D or (N/A)] N/A

CONCURRENCE SIGNATURES (Activity must be included) - RESOLVE COMMENTS BEFORE SIGNING

SIGNATURE/ACTIVITY	DATE	TYPE	DETAILS OF REVIEW REQUESTED (if necessary)

TYPE OF REVIEWS (to be determined by author) [See table at end of instructions for definitions.]

1-Peer:Summary 2-Peer:Intermediate 3-Peer:Detail 4-Independent 5-Informal Committee 6-Formal Committee 7-Specialist 8-Interface

NAME TYPED AND SIGNATURE OF NEXT HIGHER MANAGER NOT SIGNING ON LETTER — DATE

J. E. Hack John E. Hack 1/23/06

- CONTRIBUTORS AND IMPACTED PARTIES NOT REQUESTED TO CONCUR AND WHY:

DISTRIBUTION

Bettis

MN Smith, 02B/GM
SD Harkness, 01Q/MT
M Zika, 01C/SE
CD Eshelman, 36E/SE
D Hagerty, 38D/SE
RC Jewart, 01C/SE
JE Hack, 05R/MT
R Baranwal, 05P/MT
MH Krohn, 05R/MT
DC Noe, 05P/MT
JA Glass Jr., 05R/MT
RW Smith, 05R/MT

NR

DI Curtis (3), 08S **(INFO)**
JD Yoxtheimer, 08S/8034
S. Bell, 08I/8024
DE Dei, 08A/8011
WE Evers, 08E/8019
JP Mosquera, 08C/8017
TJ Mueller, 08R/8033
MD Natale, 08I/8024
CH Oosterman, 08C/8017
TN Rodeheaver, 08I/8024
SJ Rodgers, 08E/8019
SJ Trautman, 08V/8037

KAPL

MJ Wollman, 111
SA Simonson, 081
DF McCoy, 111
JM Ashcroft, 132
PF Baldasaro, 111
Y Ballout
B Campbell
CF Dempsey, 111
L Kolaya
G Newsome
H Schwartzman, 132
BM Lugert
JA Vollmer
J Beale

PNR

J Andes
HA Cardinali
JF Koury

SNR

D Clapper, 065
GM Millis, 065

BPMI-P

SD Gazarik
RF Hanson